FISH & RICHARDSON P.C.

OriiliNAL

Frederick P. Fish
1855-1930

W.K. Richardson
1859-1951

October 15, 1999

FX PARTE OR LATE FILED

By Hand Delivery

Ms. Magalie Roman Salas
Secretary
Federal Communications Commission
The Portals TW-A325
445 12th Street, SW
Washington, DC 20554

RECEIVED

OCT 1 5 1999

FEDERAL COMMUNICATIONS COMMISSION
OFFICE OF THE SECRETARY

BOSTON

DELAWARE

NEW YORK

SILICON VALLEY

SOUTHERN CALIFORNIA

TWIN CITIES

WASHINGTON, DC

Re: 1998 Biennial Regulatory Review - Amendment of Part 18 of the
        Commission's Rules to Update Regulations for RF Lighting Devices
        ET Docket No. 98-42
        Our File: 07330/008001

Dear Ms. Salas:

Please accept the following *ex parte* submissions in the above-captioned docket
which may not have been received previously by the Commission staff. These
documents represent correspondence between the parties which should be entered
into the record. The Part 15 Interests have no objection to this submission provided
it is noted that their March 2, 1999, letter has been superseded by their letter of
June 21, 1999.

1/29/99	Letter from M. Lazarus to T. Mahn
3/2/99	Letter from M. Lazarus to T. Mahn
3/12/99	Letter to M. Lazarus from T. Mahn

Very truly yours,

Terry G. Mahn

/seg

cc: Service List
        Enclosures

102554.W11

No. of Copies rec'd __0+4__
List ABCDE

SERVICE LIST

Chairman William E. Kennard
Federal Communications Commission
445-12th Street, S.W.
Room 8-B201
Washington, DC 20554

Mr. Ari Fitzgerald
Office of Chairman Kennard
Federal Communications Commission
445-12th Street, S.W.
Room 8-B201
Washington, DC 20554

Commissioner Susan Ness
Federal Communications Commission
445-12th Street, S.W.
Room 8-B115
Washington, DC 20554

Mr. Daniel Conners
Office of Commissioner Ness
Federal Communications Commission
445-12th Street, S.W.
Room 8-B115
Washington, DC 20554

Commissioner Harold Furchgott-Roth
Federal Communications Commission
445-12th Street, S.W.
Room 8-A302
Washington, DC 20554

Mr. Paul Misener
Office of Commissioner Furchgott-Roth
Federal Communications Commission
445-12th Street, S.W.
Room 8-A302
Washington, DC 20554

Commissioner Michael K. Powell
Federal Communications Commission
445-12th Street, S.W.
Room 8-A204
Washington, DC 20554

Mr. Peter Tenhula
Office of Commissioner Powell
Federal Communications Commission
445-12th Street, S.W.
Room 8-A204
Washington, DC 20554

Commissioner Gloria Tristani
Federal Communications Commission
445-12th Street, S.W.
Room 8-C301
Washington, DC 20554

Ms. Karen Gulick
Office of Commissioner Tristani
Federal Communications Commission
445-12th Street, S.W.
Room 8-C301
Washington, DC 20554

Mr. Julius P. Knapp
Chief, Policy and Rules Division
Office of Engineering and Technology
Federal Communications Commission
445 12th Street, S.W.
Room 7-B133
Washington, D.C. 20554

Ms. Karen Rackley
Chief, Technical Rules Branch
Office of Engineering & Technology
Federal Communications Commission
445 12th Street, S.W.
Room 7-A161
Washington, D.C. 20554

Mr. John A. Reed
Senior Engineer, Technical Rules Branch
Office of Engineering & Technology
Federal Communications Commission
445 12th Street, S.W.
Room 7-A140
Washington, D.C. 20554

David C. Jatlow, Esq.
Young & Jatlow
1150 Connecticut Avenue, NW
Suite 420
Washington, DC 20036

Larry Solomon, Esq.
Shook, Hardy & Bacon L.L.P.
Hamilton Square
600 14th Street, NW
Suite 800
Washington, DC 20005-2004

Mitchell Lazarus, Esq.
Fletcher Heald & Hildreth, P.L.C.
1300 North 17th Street
11th Floor
Rosslyn, VA 22209-3801

Ellen Ranard, Esq.
Fusion Lighting, Inc.
7524 Standish Place
Rockville, MD 20855

Daniel Tessler, Chairman
Fusion Lighting, Inc.
7524 Standish Place
Rockville, MD 20855

ANN BAVENDER*
ANNE GOODWIN CRUMP
VINCENT J. CURTIS, JR
RICHARD J. ESTEVEZ
PAUL J. FELDMAN
ROBERT N. FELGAR*
RICHARD HILDRETH
FRANK R. JAZZO
ANDREW S. KERSTING*
EUGENE M. LAWSON, JR
HARRY C. MARTIN
GEORGE PETRUTSAS
RAYMOND J. QUIANZON
LEONARD R. RAISH
JAMES P. RILEY
KATHLEEN VICTORY
HOWARD M. WEISS

* NOT ADMITTED IN VIRGINIA

FLETCHER, HEALD & HILDRETH, P.L.C.

ATTORNEYS AT LAW

11th FLOOR, 1300 NORTH 17th STREET

ARLINGTON, VIRGINIA 22209-3801

———

(703) 812-0400

TELECOPIER

(703) 812-0486

INTERNET

www.fhh-telcomlaw.com

FRANK U. FLETCHER
(1939-1985)
ROBERT L. HEALD
(1956-1983)
PAUL D.P. SPEARMAN
(1936-1962)
FRANK ROBERSON
(1936-1961)
RUSSELL ROWELL
(1948-1977)

EDWARD F. KENEHAN
(1960-1978)

CONSULTANT FOR INTERNATIONAL AND
INTERGOVERNMENTAL AFFAIRS
SHELDON J. KRYS
U. S. AMBASSADOR (ret.)

OF COUNSEL
EDWARD A. CAINE*
MITCHELL LAZARUS*
EDWARD S. O'NEILL*
JOHN JOSEPH SMITH

WRITER'S DIRECT

(703) 812-0440

January 29, 1999

Terry G. Mahn, Esq.
Fish & Richardson, P.C.
601 13th Street, N.W.
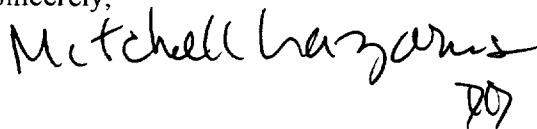Suite 500 North
Washington, D.C. 20005

Dear Terry:

As agreed in our meeting on January 14, I am enclosing technical materials on 2.4 GHz spread spectrum systems and their susceptibility to interference, with a cover memo from Jim Zyren of Harris Corporation.

I join in Jim's request for Fusion's cooperation in obtaining release of the OET test data on Fusion's product.

I hope this material is helpful, and look forward to resuming discussions with you and your client. Please do not hesitate to call with any questions in the meantime.

Sincerely,

Mitchell Lazarus

Enclosures
cc: (w/out enclosures):
David Jatlow, Esquire
Ray Martino, Symbol Technologies, Inc.
Carlos Rios, 3Com Corporation
Larry Solomon, Esquire, Counsel for Metricom
Jim Zyren, Harris Corporation

To: Fusion Lighting   1/29/99

Fr: Jim Zyren, Harris Semiconductor

Re: Information requested by Fusion Lighting

In regard to the meeting between Part 15 interests and Fusion Lighting on January 14, 1999, I am forwarding information describing the performance characteristics of IEEE 802.11 wireless LAN radios. This data includes the standard to which this equipment conforms as well as descriptions of the impact on WLAN reliability of RF interference generated by magnetron sources in consumer microwave ovens.

1.) IEEE Std 802.11-1997: IEEE Standard for Wireless LAN Medium Access Control (MAC) and Physical Layer (PHY) specifications

2.) Horne, J. and Vasudevan, S., "Modeling and Mitigation of Interference in the 2.4 GHz ISM Band", *Applied Microwave & Wireless*, March / April 1997, pp. 59-71.

3.) Zyren, J., "Effects of Microwave Oven Interference on IEEE 802.11 WLAN Reliability", IEEE P802.11 - 98/240, May 1998.

In addition to the data described above, alternative proposals for in-band emission limits and limiting emissions to some portion of the 2.45 GHz ISM band in order to promote spectrum sharing are being considered by the Part 15 interests. We would like to point out that ISM devices operating in accordance with Part 18 of the Commission's rules can use the entire ISM band from 2400 - 2500 MHz. By comparison, Part 15 devices are limited to 2400 - 2483.5 MHz.

In order to facilitate our understanding of RF lighting devices, I would like to reiterate our request for release of the FCC test data gathered on the device Fusion provided to OET for evaluation as part of this proceeding. Due to the fact that RF lighting devices operating in the 2.45 GHz ISM band are not generally available for purchase, release of test data gathered by OET would expedite discussion between the parties.

Modeling and Mitigation of Interference in the 2.4 GHz ISM Band

This article presents the results of investigations into the nature of interference sources in this band and discusses methods for minimizing their effects on communication links

By Jonathan Horne, University of Colorado
S. (Vasu) Vasudevan, Ph.D., US WEST Advanced Technologies

Three frequency bands at 900 MHz, 2.4 GHz, and 5.7 GHz are among those that have been designated in the United States as Industrial, Scientific and Medical (ISM) bands. In these bands, radio communication using spread-spectrum techniques is permitted without license requirements, subject only to equipment type approval and additional Effective Isotropic Radiated Power (EIRP) and processing gain requirements. Interference from extraneous sources (unintentional radiators) impacts the reliability of communication in each of these bands. In the case of the 2.4 GHz ISM band, the dominant sources of such interference are the 80 million residential microwave ovens radiating at a nominal frequency of 2.45 GHz. The ubiquity of these ovens and the wideband interference picture that emerges from peak-power measurements using, for example, conventional spectrum analyzers in max-hold mode, has sometimes led to pessimistic conclusions about the possibility of sustaining high-reliability communication links in this band. Therefore, in this paper we develop some insights into the nature of these predominant interference sources in the 2.4 GHz band, discuss their impact on communication link reliability and outline strategies for minimizing the effects of such interference.

We begin with an overview of the nature of telephony applications in this band and discuss the potential for disruption of communication links by interference from microwave ovens, followed by a review of prior work done on characterizing these interferers. That leads to a discussion of more recent measurements, revealing a clearer picture of these emitters' behavior. These results are then developed into a simple analytical model to provide greater understanding of previously reported experimental observations. The enhanced understanding of emission characteristics gives us additional basis on which to plan deployments. While careful deployment planning is a viable short-to-medium term strategy, a permanent solution to such interference related problems necessarily must involve modifications to the system itself. Therefore, we present some promising approaches for excising and hence gaining robustness to this type of interference.

Telephony applications

The radio equipment available for 2.4 GHz ISM band operation includes point-to-point as well as point-to-multipoint systems, for indoor and outdoor applications. The outdoor deployments can be used either to set up transmission links to subscriber clusters followed by wired distribution or to provide telephone service via direct wireless drops to customers. Indoor applications would include wireless LANs and dual-mode PCS/cordless phones (which may operate in the 2.4 GHz band indoors).

In each of these applications there is a potential impact from the unintentional radiators in the band. According to the measurements performed on a sampling of microwave ovens by Gawthrop et al. [1, 2], the maximum EIRP of these radiators lay between 16 to 33 dBm while the average EIRP was around 5 dBm. While this gives communication systems operating at an EIRP of 36 dBm (the maximum allowed by the FCC) a significant power advantage, it can be wiped out if the interference sources are closer to the receiver and within the receiver's field of vision.

From the preceding facts it is clear that when viewed from the perspective of EIRP alone, microwave oven emissions have the potential to degrade communication links. The extent to
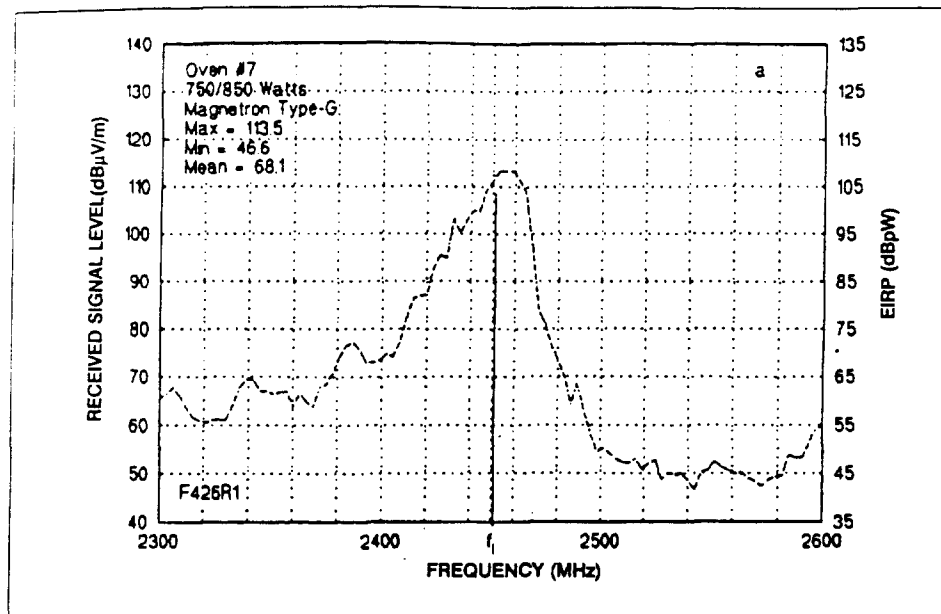
■ Figure 1. Representative frequency-domain spectrum analyzer peak power (max-hold) measurement trace reported by NTIA.

which such interference impacts system reliability and the extent to which it can or needs to be combated depends on the characteristics of the interference as well as the particular application, and motivates our investigation of the issues.

Microwave oven emissions

The National Telecommunications and Information Administration (NTIA) measured individual microwave oven emissions to ascertain the usability of the 2.3-2.5 GHz bands for radio communication. These measurements, summarized in two technical reports [1, 2], are extensive and have been made in both frequency- and time-domains. The frequency domain measurements (Figure 1) have been made with spectrum analyzers in max-hold mode and the resulting traces capture the peak emission that has

occurred at any instant within the time interval of observation at each frequency sampling point.

The time domain measurements (Figure 2) are zero-span traces on the spectrum analyzer and reveal the signal power within a certain frequency band over time.

While the NTIA cautions against pessimistic conclusions regarding the emission characteristics based on the peak spectrum measurements and additionally supplement the frequency-domain characterizations with time-domain plots to demonstrate its pulsed nature, they do not explicitly specify a time-frequency characteristic for these emissions.
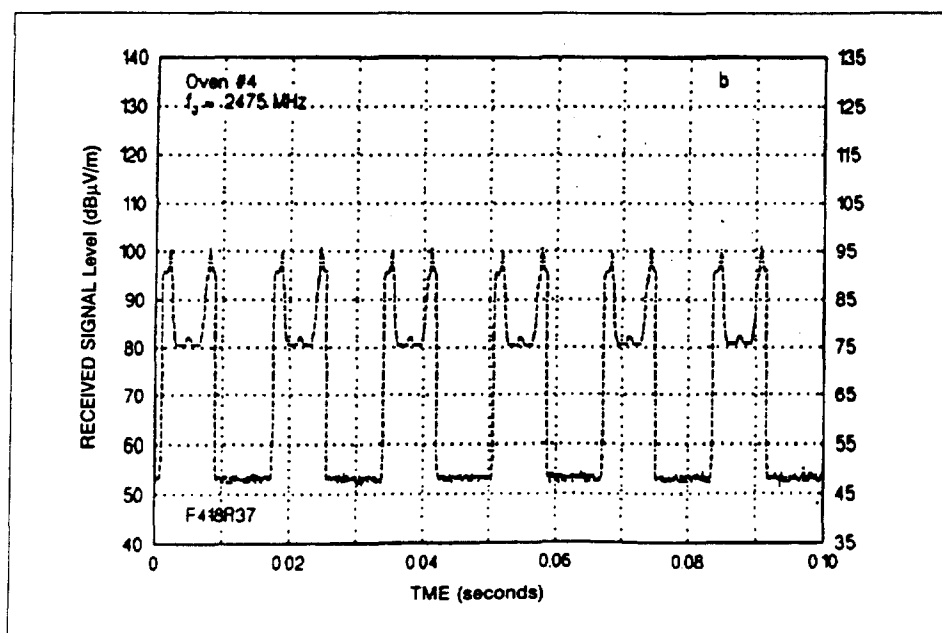
Time-frequency characterization

Emissions from a sample oven were recorded on the TEK 3054, a real-time digital spectrum analyzer, at the Tektronix facility in Irvine to clarify this issue. The spectrogram display of this instrument with updates at real-time rates allows for a relatively straightforward identification of variations in the frequency content of the input signal with time. One of the resulting traces, with frequency and time along the x- and y-axes respectively and gray-scale coded signal-amplitude representation, is presented in Figure 3, revealing the time-frequency relationship of these emissions.

The previous observations are key. Not only do they confirm that the emissions leaking from microwave ovens are essentially narrow-band, albeit with significant frequency wander; they also exhibit the general nature of this movement in frequency. The knowledge of this structure opens up the possibility of being able to actually combat such interference and mitigate its effect on communication devices operating in the 2.4 GHz ISM band.
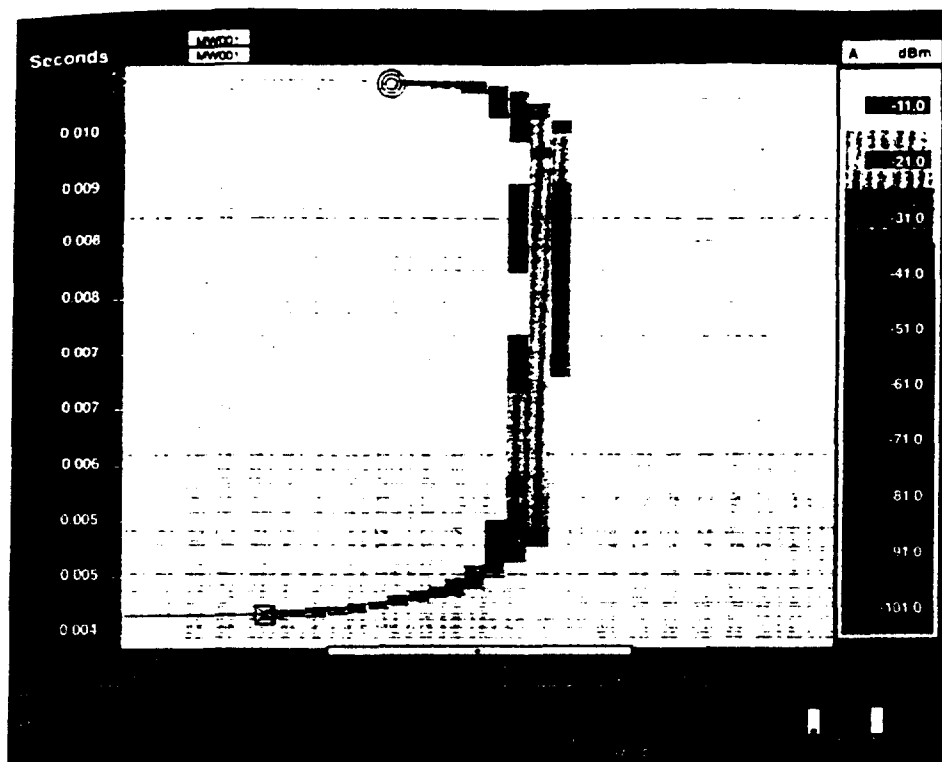
An analytical emission model

The frequency characteristic of the trace of Figure 3 can be described as a phase modulation of an RF carrier. To accommodate amplitude variations in the observed signal, an amplitude modulation needs to be superimposed on this

■ Figure 2. Representative time-domain signal measurement reported by NTIA.

■ Figure 3. Emission time-frequency characteristic over a single power cycle.

cy ω_c is phase modulated by $p(t)$ and amplitude modulated by $a(t)$. In the simplest case $a(t)$ is a rectangular pulse waveform of duration equal to the on-time of the oven magnetron and $p(t)$, a sinusoid at 60 Hz.

While the above model needs both additional validation as well as refinement, the picture it presents is useful in conceptualizing the nature of the interference. To illustrate some of these refinements, consider first the fact that the carrier frequency previously has been reported to drift. This drift can be easily accommodated by introducing a time-dependence on ω_c. Further, the amplitude function $a(t)$ can be used not only to switch the interference on and off but also to vary the amplitude of the emission during the on-period. Next, additional harmonics can be introduced in $p(t)$. Finally, a wide-band noise smear is sometimes seen at the switch-off times of the magnetron. This can be represented in our model as a sudden drop to zero of the modulating waveform at these instants.

Purely time-domain or frequency-domain observations

It is instructive to examine some of the NTIA reported emission features in the context of our observations. In Figure 4, we relate the time-frequency characteristics of a signal to purely time- or frequency-domain measurements made on a conventional spectrum analyzer.

As shown, the time-domain (zero-span) plots can be derived by taking a vertical slab of the time-frequency characteristic. Analogously, the peak frequency (max-hold) measurements can be seen as the projection of a horizontal slab of this characteristic, onto a plane.

Considering first the time-domain plots reported by the NTIA, we note the pulses in these plots are, in fact, not constant in amplitude with a significant dip over the pulse interval for most of the ovens. Such a snapshot is completely consistent with a vertical slice of Figure 3 within the range of the signal's instantaneous frequency swing, and corresponds to the 'rabbit ears' mentioned in the NTIA reports. Further, the reason

PM carrier. Such a model offers the flexibility to generate the most significant features of the interference through a simple variation of parameters. Formally, we express the interference signal $i(t)$ as
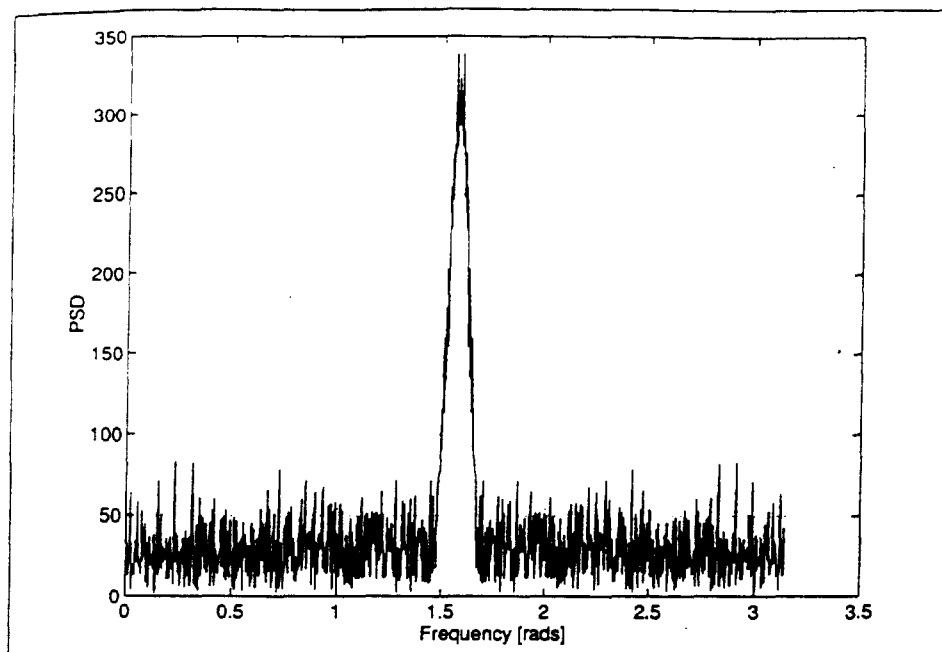
$$i(t) = a(t)\cos(\omega_c t + k_p p(t))$$

where the carrier at radian frequen-
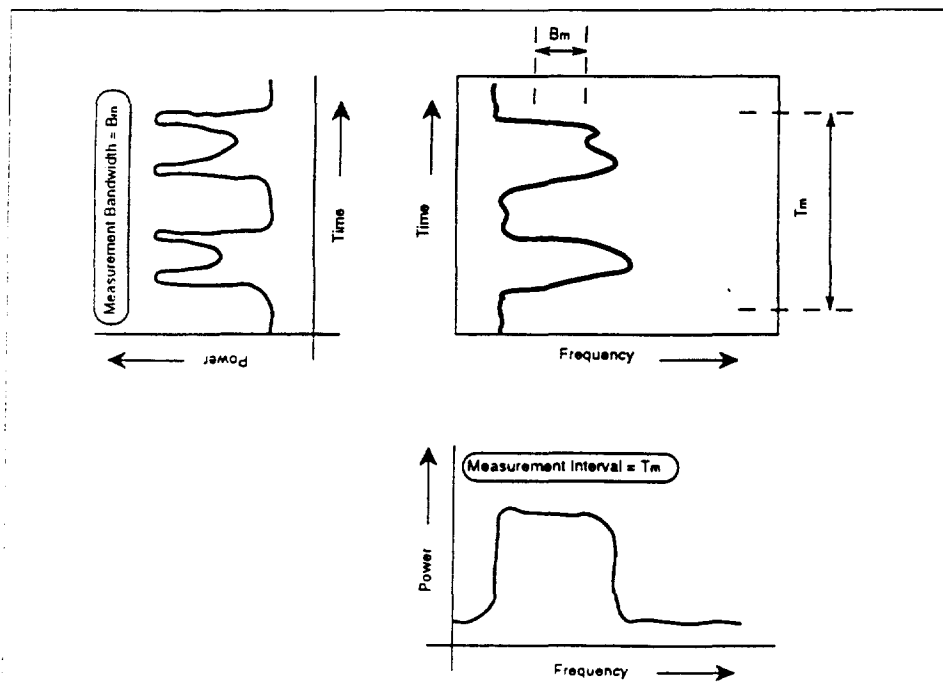
■ Figure 4. Relating time- and frequency-domain measurements to actual signal time-frequency characteristics.

■ Figure 5. Narrow-band interferer on white (broadband) signal.

for the fill-in of the pulses as the measurement bandwidth for the time-domain measurements is increased, also now is made clear. Increasing this bandwidth results in capturing a greater percentage of the signal as it swings over a frequency range.

As far as the max-hold plots are concerned, the time-frequency characteristic explains some of the signal frequency-spread about the 2.45 GHz nominal carrier. The spread also may be compounded by carrier-frequency drift. The wide-band smears that occasionally are produced by the oven during the ends of each power cycle could partly account for the rise in the overall noise floor.

Mitigating the impact of microwave oven interference

One of the principle advantages of spread-spectrum communications is its relative immunity to narrow-band jammers and noise. Indeed, many low data-rate systems such as cordless telephones, can employ a processing gain which is large enough to overcome all but the most tenacious interferers. For such applications, the added cost of excision techniques may outweigh any performance improvements. On the

other hand, high data-rate applications are constrained in bandwidth and therefore cannot afford the luxury of excessive processing gains. Increased noise power means decreased capacity, so anything that can be done to decrease interference will be of interest.

The first steps to interference mitigation are familiar and easily categorized as "deployment planning." These include proper band selection for a given geographical region as well as the use of directional and sectorized antennas. Power restrictions must be weighed against the presence of harmful interferers and available bandwidth. For mobile installations, much of this information may remain unknown *a priori*, and in an urban environment, even complete knowledge of the RF environment may not allow for sufficient interference attenuation.

A more aggressive approach to combating interference involves altering the transmission format (including modulation and coding) and/or introducing additional signal processing at the receiver. Known interferers, such as a pure-tone jammer, are easily avoided through techniques such as selective frequency-hopping, or attenuated, at the

expense of a small signal loss, through the use of a properly tuned notch filter. In fact, interferers which can be reasonably modeled by a low-order stochastic process can be dealt with quite elegantly through the use of parametric filtering techniques. See the discussions on Narrow-Band Interference Rejection by Masry [3], by Ketchum and Proakis [4], or by Hsu and Giordano [5].

Transform domain filtering

Microwave interferers, along with many others, are harder to model statistically. The interference comes and goes as ovens are turned on and shut off, varies in strength and wanders about in frequency. In sum, the best filtering technique for this type of interference will be a non-parametric one. In order to distinguish the microwave signal from the information-bearing one, we exploit what little information we have; in particular, the spread-spectrum signal, henceforth assumed to be direct-sequence, closely resembles white Gaussian noise while the microwave interferer is narrow-band (over some time interval).

Assume for the moment that the interference exhibits no frequency wander. That is, it closely resembles a pure tone whose frequency remains constant through time. Then, if the received interference power is strong enough, we expect to see an appreciable spike in the frequency domain version of the received signal, comparable to the one shown in Figure 5.

An intuitively appealing filtering technique is to find such a frequency domain representation of the received signal, replace spectral components which obviously belong to the interference with zeros and invert the transform. Although some of the desired signal is lost in this operation, it would seem that under the right circumstances this loss will be countered by significant signal-to-noise ratio gains and a corresponding drop in BER. The proposed idea is shown in Figure 6.

This technique, known as transform domain filtering (TDF), is not new. Some of the earlier work such as that of [6], uses surface acoustic
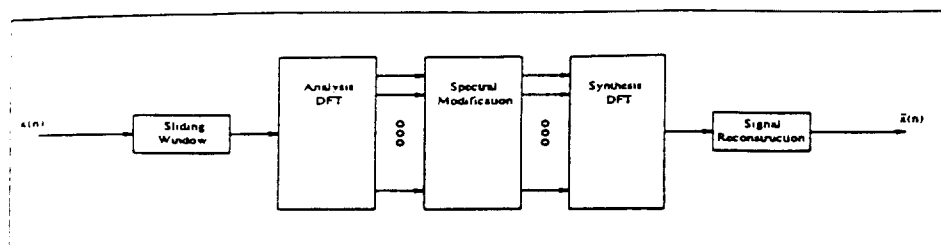
■ Figure 6. Discrete Fourier transform (DFT) analysis-modification-synthesis.

wave (SAW) devices to generate real-time Fourier transforms. In continuous time, the author computes expressions for the filter output and introduces a technique to avoid ISI. Gevargiz et al. [7] study both SAW and DFT techniques with which they perform TDF by using adaptive notch filters and soft limiting.

One of the primary problems we encounter with TDF is discerning signal from (interference) noise and deciding at what point filtering will improve system performance. Notching out bins in the frequency domain is equivalent to multiplying the received spectrum by a filter whose spectrum is white except for nulls at notch points. Clearly, deep notches (mandated by a low SNR) imply a large filter impulse response, resulting in more inter-symbol interference. At the opposite

extreme (high SNR), it makes little sense to apply filtering because any notching will eliminate significantly more signal than noise.

Short-time Fourier transform

Short-time transform techniques are most relevant when the interferer is non-stationary. Technically this means that the statistics underlying a random process which adequately describes the interferer change with time. This is reflected in the corresponding signal in a variety of ways including a change in mean amplitude, instantaneous frequency or waveform shape. In this case, it is important to localize the interference signal energy in frequency and time, the latter being a task ideally suited to a sliding analysis window. Figure 7 demonstrates this technique for a simple chirp signal and a

Hamming analysis window. By multiplying the (presumably) infinitely long signal by a finite length sequence, all information except that lying inside the window is discarded, and we have a 'short-time' signal.

If we choose an appropriate analysis window of proper length, we can ensure quasi-stationarity. That is, the nature of the interference does not change significantly over the duration of the window. Then the Fourier transform of the windowed signal approximately represents an instantaneous spectrum and is known as the Short-Time Fourier Transform (STFT). Though derived as a continuous transform which maps a continuous time-domain signal to a continuous combined time-frequency domain signal, it shares the same variations as the Fourier transform. Namely, it may be discrete and/or periodic in one or both domains. Of particular interest is the STFT which is periodic in time and frequency and therefore easily realized with the DFT.

It should be noted that for an approximately sinusoidal interferer such as the microwave oven, projection onto the Fourier basis provides a high degree of separation of signal from noise. Other bases may prove more valuable for different interferers. Further, alternate bases may be selected such as the Walsh-Hadamard transform [12] which are binary, real-valued functions and hence computationally less expensive. The use of such bases allows one to trade performance for complexity.

Among previous publications on the use of the STFT, Portnoff's [8] is comprehensive and referred to in much recent literature. He reviews all of the fundamentals of the STFT and discusses such problems as performing time-varying filtering through modifications in the time-frequency domain. Allen's [9] predates Portnoff's and presents some similar STFT results, including a study of the effects of filtering in the transform domain. Ketchum and Proakis [4], along with other techniques, propose the use of averaged periodograms (the Welch method) to create a time-varying whitening fil-
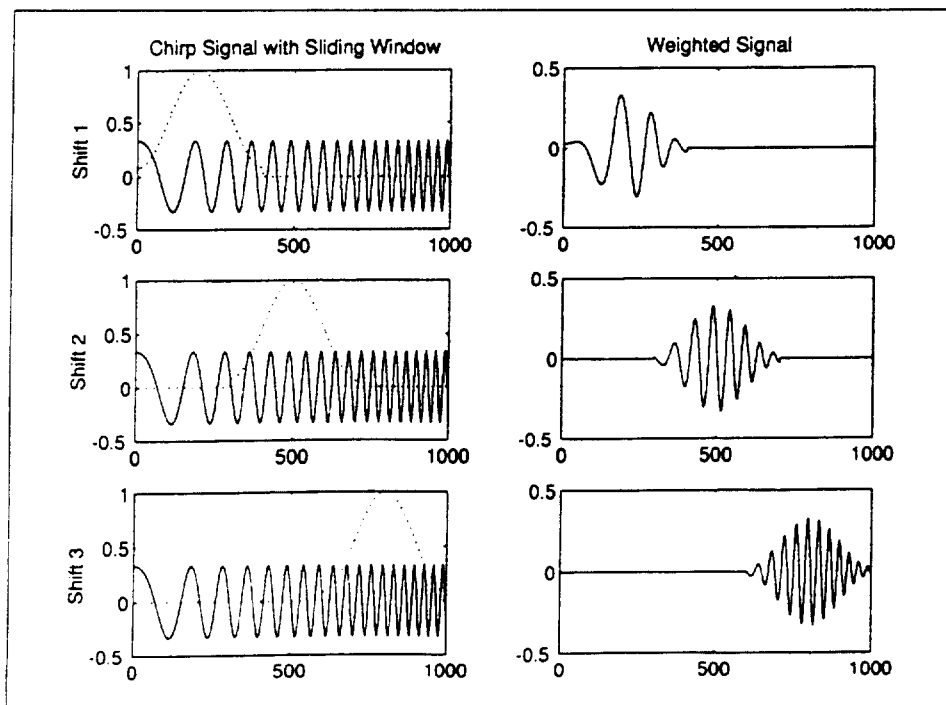
■ Figure 7. Using a Hamming window to obtain quasi-stationarity.
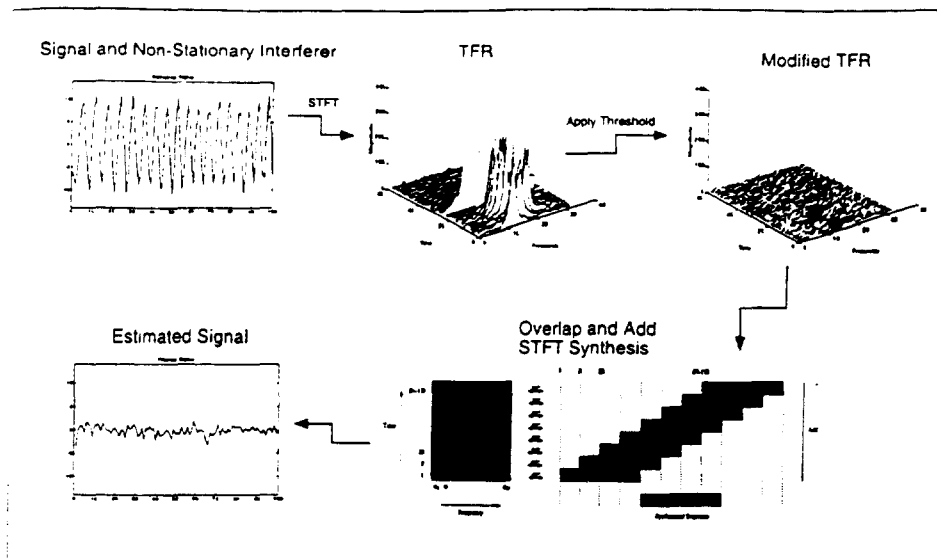
■ Figure 8. Interference excision process.

ter in the spectral domain. Rabiner and Schafer [10] discuss the STFT as applied to speech processing, and Crochiere and Rabiner [11] discuss STFT techniques in the context of multirate digital signal processing.

Transform domain filter application

The underlying ideas behind transform domain filtering are well understood, and the necessary tools for realizing such a non-parametric filter, namely the STFT analysis and synthesis relations, are at our disposal. Implementation is application-dependent, however, so our algorithms will need to be further refined for use with the microwave interferer. The goal of this section is to develop criteria for optimal transform domain filter performance in the context of a direct-sequence spread-spectrum communications system.

Of primary concern are the analysis window, the short-time transform parameters and the associated filtering techniques. Our implementation of the interference excision process is shown in Figure 8.

Analysis window

With any short-time transform, the shape and length of the analysis window will have a direct impact on the spectral estimate of the time-varying signal. The discrete time STFT $X_n(e^{ju})$ of a discrete-time sequence $x(n)$ can be thought of as the normal discrete time Fourier transform of the windowed sequence $w(n-m)x(m)$, and hence

$$X_n\left(e^{j\omega}\right) = \frac{1}{2\pi} \int_{-\pi}^{\pi} W\left(e^{-j\theta}\right) e^{-j\theta n} X\left(e^{j(\omega-\theta)}\right) d\theta$$

where

$$X\left(e^{j\omega}\right) = \sum_{m=-\infty}^{\infty} x(m) e^{-j\omega m}$$

$$W\left(e^{j\omega}\right) = \sum_{m=-\infty}^{\infty} w(m) e^{-j\omega m}$$

It becomes clear that the effect of the window is to low-pass filter in the frequency domain. The result of this blurring is decreased frequency resolution. Consequently, the larger the bandwidth of the analysis window, the poorer the interference frequency localization. This works as a general rule of thumb, but more factors determine a specific window's applicability to a given problem. Considerations include: equivalent noise bandwidth (ENBW), processing gain (PG), overlap correlation, scalloping loss, worst case processing loss (PL), spectral leakage and minimum resolution bandwidth. All of these are discussed in detail by Harris [13] but largely omitted here. Instead, we use his results to draw two important conclusions: First, a rectangular window has large side-lobes that will significantly alter our spectral estimate. Second, a tapered window such as the Hamming window, has smaller side-lobe levels but a wider main-lobe, which effectively
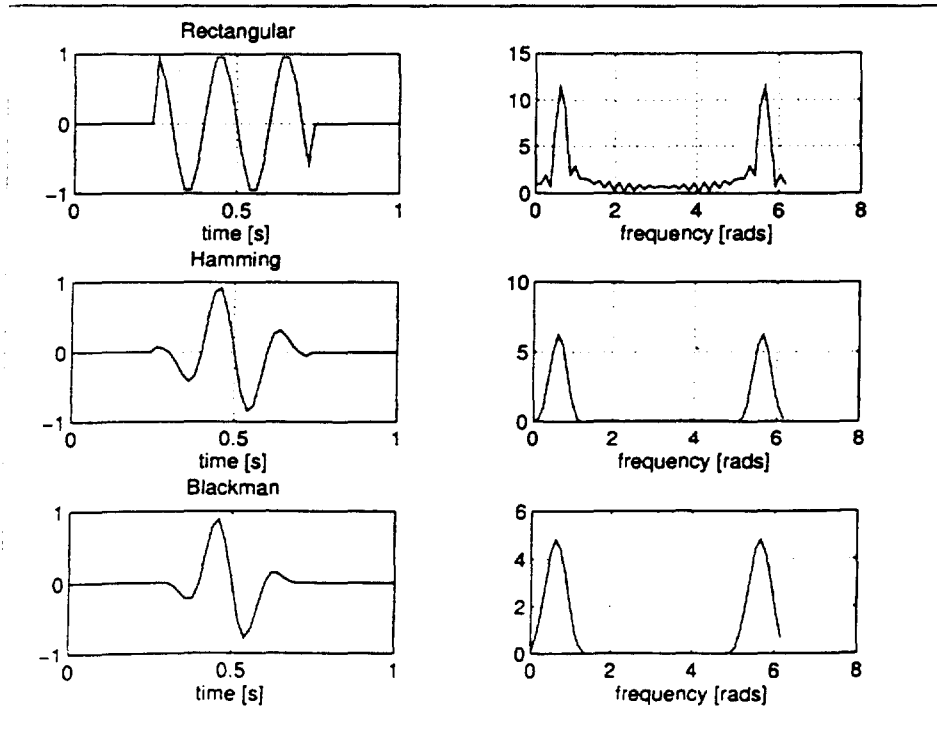
■ Figure 9. Comparison of some common window functions.

decreases the spectral resolution and reduces the spectral distortion. This is shown in Figure 9 which compares three common analysis windows. Non-overlapping tapered windows risk losing part of the signal at the window edges, but for our purposes we will always overlap the windows (thereby nullifying this risk). We note that any reasonable window will allow for perfect reconstruction from the TFR, but the best window will maximize separation of signal from interference in the time-frequency domain.

The window length is inversely proportional to its bandwidth, so there is a fundamental tradeoff between time and frequency resolutions. The absolute lower bound to the time-bandwidth product known as the 'uncertainty principle,' states that for a time-width T measured in seconds and bandwidth B measured in Hertz, the product $T \cdot B \geq 1$. A proof based on the Cauchy-Schwarz inequality can be found in [14].

Optimal window length

As we lengthen the analysis window, we compromise temporal localization for frequency localization. It stands to reason that the optimal window length lies somewhere between two extremes. Indeed, this length is a function of the analysis window used and of the nature of the interference to be filtered.

For the analysis, some simplifying assumptions are needed. Namely, the interferer is assumed to be a sinusoid whose instantaneous frequency increases at a constant rate v. Further, we assume our TDF is based on the STFT using N-point DFT's. The signal is sampled at f_s Hz. The L-point analysis window is assumed to be band-limited to B Hz. Hence the sinusoid's total change in frequency over the duration of the analysis window is given by

$$\Delta freq = v \cdot \left(L \frac{1}{f_s} \right)$$

Note that, as time progresses, the interferer energy will be concentrated in increasingly higher frequency bins. Let time $t = 0$ correspond to a

moment when a previously occupied frequency bin has just emptied and all of the interferer energy now occupies higher frequency bins. For simplicity, let this time also be the beginning of the current analysis window.

Assuming the number of points in the DFT equals the window length $(N = L)$, the best we can do is find an L which constrains the frequency spread to as few bins as possible. This is slightly different from minimizing the spread in frequency because there may be a non-minimum frequency spread which occupies the same number of bins as the minimum spread but has a correspondingly larger L. However, because we can change the size of the frequency bins by arbitrarily increasing N (note that the frequency resolution is not increased by doing this!), the two problems are essentially the same. We tackle the easier of the two.

The number of occupied frequency bins is

$$\text{no bins} = \left\lceil \frac{2BLf_s + vL^2}{f_s^2} \right\rceil$$

and we opt to minimize the frequency spread,

$$L_{opt} = \min_L \left(2B + v \frac{L}{f_s} \right)$$

Consider the specific example of a rectangular pulse. A rectangular analysis window of duration $T = L/f_s$ has a main lobe bandwidth (determined by the first zero-crossings) of $1/T$ Hz, or equivalently $B = f_s/L$. By simple calculus,

$$L_{opt} = \sqrt{\frac{2f_s^2}{v}}$$

Now consider the Hamming window of time-width $T = L/f_s$ and main lobe bandwidth $B = 2f_s/L$. Calculated as above,

$$L_{opt} = \frac{2f_s}{\sqrt{v}}$$

Window overlap

The first step in obtaining the STFT is to window the time signal every R samples to yield

$$x_{win}(n) = x(n)w(rR - n)$$

This corresponds to sampling the TFR in the time-dimension every Rth sample. Thus decreasing R, which corresponds to increasing the window overlap, effectively will increase the TFR temporal sampling frequency.

Using the STFT overlap-and-add synthesis technique, we see that as R gets smaller, more windows must be overlapped to reconstruct equal length time intervals. Adding the overlapped windows together is comparable to averaging them. Thus, the variance of the spectral estimate is decreased in direct proportion to R. The maximum overlap permitted is limited only by the length of the analysis window itself and the computational complexity/storage requirements involved with larger TFR's.
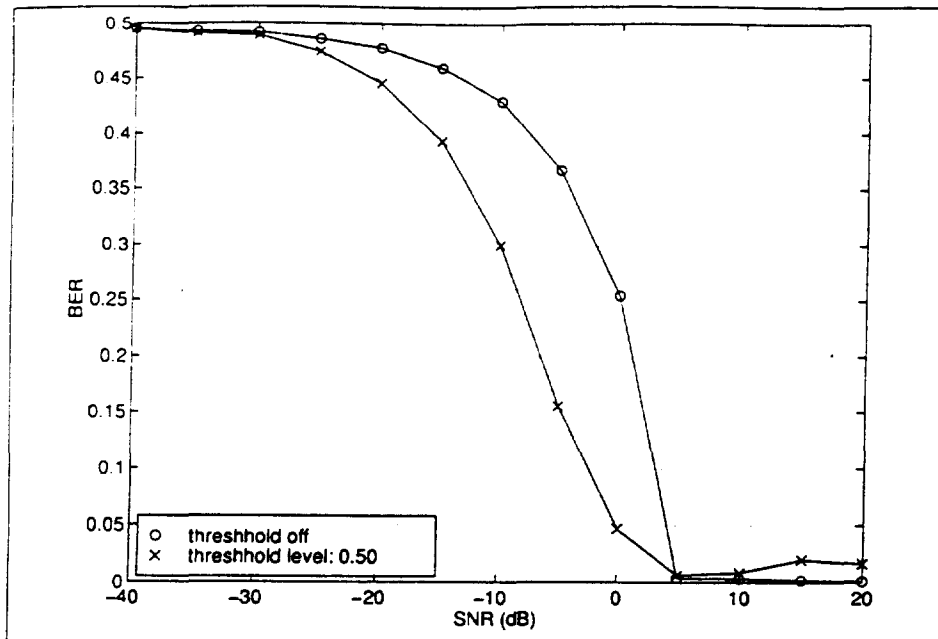
Thresholding

The previous section briefly mentioned the idea of transform domain thresholding. With this technique, we find a time-frequency representation of the signal of interest, and set any spectral component which exceeds some threshold to zero. The choice of optimal threshold is not an obvious one, but we have some intuitive ideas about how it works. As in all the other analysis in this paper, we assume that the signal is comprised of an essentially white broadband information signal and a narrow-band non-stationary interferer.

If the signal power is large compared to that of the interferer, then it is clear that the threshold also should be large. Otherwise, we risk excising the information signal along with the interferer. If the signal power is small relative to the interference power, then it makes sense to have a smaller threshold. That way we are sure to remove most of the interference with minimal impact on the information signal.

As discussed above, we know that performing this thresholding opera-

■ Figure 10. BER as a function of SNR for filtered and unfiltered signals (Threshold = 0.5).

tion is equivalent to convolving with some time-varying filter in the time-domain. Thus, by filtering in this manner, we introduce inter-symbol interference (ISI). A deeper notch in the spectral domain (due to zeroed spectra) corresponds to a larger filter. A larger filter means more significant ISI. Thus, we have a trade-off. Not only must we consider the balance between noise and signal power, we must examine the effect of ISI due to filtering.

One way to avoid ISI completely is to examine the received signal bit by bit. Assuming the receive clock is synchronized with the transmit clock, we know where each bit interval starts and ends. We can then do filtering over a particular bit interval without distorting surrounding bits with ISI. This places a restriction on our window size, and therefore may not always work, or may at least be sub-optimal. In fact, if the processing gain is too small, there will not be enough chips for each bit to provide adequate frequency resolution.

In prior work, Lops et al. [15] suggest the use of a separate threshold D_m for each frequency bin $m = 0...N-1$. The thresholds are chosen by constraining the conditional probability that a sample is nullified when

there is, in fact, no narrow-band interference present, i.e.

$$Pr\left(|R_m| > D_m | I = 0\right) = p, m = 0,...,N-1$$

where R is the spectrum of the received signal, and I is the interferer spectrum. They argue that this detector achieves optimal performance in that the signal loss due to excision is negligible for any value of error probability. Another idea proposed by DiPietro [16] is to excise a fixed percentage of bins or total interference power. He omits development, but this appears reasonable as long as the interferer is present.

Verification by software simulation

Because of its non-linearity and strong dependence on an unknown interferer, an optimal transform domain filter is difficult to obtain in an analytic fashion. Instead, we resort to computer simulations to illustrate some of the benefits of this technique.

The structure of the simulations is simplified; the receiver sees a random, binary, antipodal signal (which in practice would likely be binary data modulated with a PN sequence) summed with additive white Gaussian noise and a narrow-band interferer based on the model pre-

sented in the section on microwave oven emissions. In the examples below, we also have assumed unity processing gain so that chip and bit error rates coincide. The receiver creates a normalized time-frequency representation (TFR) of the received waveform using the STFT, where the largest spectral component has unit magnitude and all others are scaled linearly, and sets to zero all spectral components which exceed the specified threshold. The modified TFR then is inverted to produce an estimate of the information signal of interest. The experiment is performed over a range of SNR's and repeated several times to reduce the variance of the estimated error. Figure 10 shows the results for the case where AWGN is omitted and a threshold of 0.5 is used.

The results are better for a larger range of SNR's if we choose the threshold more carefully. Figure 11 shows the same results for a normalized threshold of 0.2.

These results indicate that transform domain filtering can markedly improve performance of a spread-spectrum receiver working in this type of environment. In Figure 11, for example, we see an improvement of nearly 18 dB at a chip error rate of 0.25. What is not shown by these plots is that the gains are dependent on a number of factors including the strength of the interferer, its instantaneous bandwidth and frequency agility, on the strength of the signal, and on algorithm parameters such as window length, window overlap, choice of TFR and threshold selection. Some of these details are discussed in [12].

Conclusion

The capacity of a spread-spectrum data link operating in the 2.4 GHz ISM band is limited by the presence of interferers, among which microwave ovens rank most prominently. A detailed study of individual ovens has revealed their emissions to be narrow band but non-stationary and therefore good candidates for adaptive filtering in spread-spectrum receivers. We introduced the idea of transform domain filtering and developed a particular
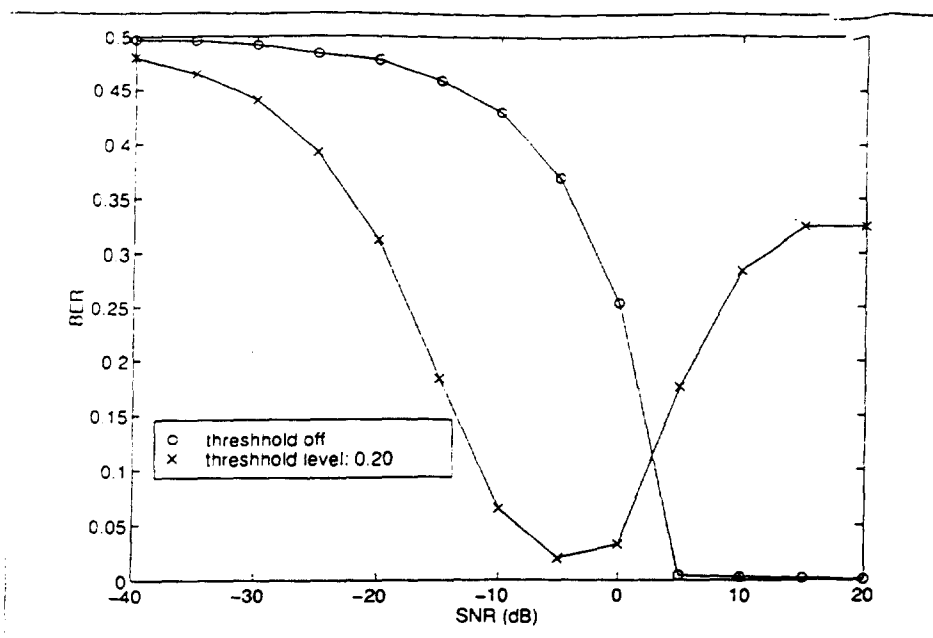
■ Figure 11. BER as a function of SNR for filtered and unfiltered signals (Threshold = 0.2).

implementation based on the short-time Fourier transform. Computer simulations based on this approach point to reasonable performance gains. ■

Acknowledgments

The authors wish to thank Tektronics for permission to use the TEK 3054 time-frequency characterization of microwave oven emissions included in this paper. The experiment was set-up and the plots generated by Kevin Cassidy, senior application engineer, federal sales and marketing group at Tektronix.

The participation of Jonathan Horne on this project was supported in part by a grant from the Colorado Advanced Software Institute.

Author information

Jonathan Horne was with the University of Colorado and now is with Qualcomm, Inc. He has worked on developing software for a number of applications including a wireless planning tool.

Subramanian Vasudevan is with US WEST Advanced Technologies in Boulder, CO. His research interests and consulting are in the general area of wireless communications with an emphasis on spread-spectrum technology. He can be reached

by e-mail at vasudeva@ecentral.com.

References

1. P. E. Gawthrop, F. H. Sanders, K. B. Nebbia, J. J. Sell, "Radio Spectrum Measurements of Individual Microwave Ovens," NTIA Report 94-303-1.

2. P. E. Gawthrop, F. H. Sanders, K. B. Nebbia, J. J. Sell, "Radio Spectrum Measurements of Individual Microwave Ovens," NTIA Report 94-303-2.

3. E. Masry, "Closed-Form Analytical Results for the Rejection of Narrow-Band Interference in PN Spread-Spectrum Systems — Part I: Linear Prediction Filters," *IEEE. Trans. Comm.*, Vol. COM-32, No. 8, August 1984.

4. J. W. Ketchum and J. G. Proakis, "Adaptive Algorithms for Estimating and Suppressing Narrow-Band Interference in PN Spread-Spectrum Systems," *IEEE Trans. Comm.*, Vol. COM-30, May 1982.

5. F. M. Hsu and A. A. Giordano, "Digital Whitening Techniques for Improving Spread Spectrum Communications Performance in the Presence of Narrowband Jamming and Interference," *IEEE Trans. Comm.*, Vol. COM-26, February 1978.

6. L. B. Milstein, and P. K. Das, "An analysis of a Real-Time Transform Domain Filtering Digital Communication System — Part I: Narrow-Band Interference Rejection," *IEEE Trans. Comm.*, Vol. COM-28, No. 6, June 1980.

7. J. Gevargiz, P. K. Das, and L. B. Milstein, "Adaptive Narrow-Band Interference Rejection in a DS Spread-Spectrum Intercept Receiver Using Transform Domain Signal Processing Techniques." *IEEE Trans. Comm.*, Vol. 37, No. 12, December 1989.

8. Michael R. Portnoff, "Time-Frequency Representation of Digital Signals and Systems Based on Short-Time Fourier Analysis," *IEEE Trans. on Acoust., Speech, and Signal Processing*, Vol. ASSP-28, No. 1, February 1980.

9. J. B. Allen, "Short Term Spectral Analysis, Synthesis, and Modification by Discrete Fourier Transform," *IEEE Trans. on Acoust., Speech, and Signal Processing*, Vol. ASSP-25, No. 3, June 1977.

10. L. R. Rabiner, and R. W. Schafer, *Digital Processing of Speech Signals*, Prentice-Hall, Inc. 1978.

11. R. E. Crochiere, and L. R. Rabiner, *Multirate Digital Signal Processing*, Englewood Cliffs: Prentice-Hall, Inc. 1983.

12. J. E. Horne, "Estimation and Excision of Non-Stationary Narrow-Band Noise with Applications to Spread-Spectrum Communications," Master's Thesis, Univ. of Colorado, December 1996.

13. Fredric J. Harris, "On the Use of Windows for Harmonic Analysis with the Discrete Fourier Transform," *Proceedings of the IEEE*, Vol. 66, No. 1, January 1978.

14. Samir S. Soliman, and Mandyam D. Srinath, *Continuous and Discrete Signals and Systems*, Prentice-Hall, 1990.

15. M. Lops, G. Ricci, and A. M. Tulino, "Robust Multi-user Detection for Synchronous CDMA Systems," CISS, Princeton, NJ, 1996.

16. Robert C. DiPietro, "An FFT Based Technique for Suppressing Narrow-Band Interference in PN Spread Spectrum Communication Systems." IEEE ICASSP'89.

Submission to
IEEE P802.11
Wireless LANs

Title: Effects of Microwave Interference On IEEE 802.11
                    WLAN Reliability

Date: May 1998

Author: Jim Zyren
                                   Harris Semiconductor
                                   jzyren@harris.com

Abstract

The influence of microwave oven interference on IEEE802.11 Wireless Local Area Network (WLAN) performance is a significant factor because they share common spectrum in the 2.400 - 2.4835 GHz Industry, Science, and Medicine (ISM) band. FCC regulations permit radiated power of up to 1 watt in this band provided spread spectrum techniques are employed. Spread spectrum methods facilitate multiple users sharing the same spectrum in an unlicensed environment and offer interference rejection properties. There are two spread spectrum techniques addressed by FCC regulations (15.247). These are Direct Sequence Spread Spectrum (DSSS) and Frequency Hopped Spread Spectrum (FHSS). Because of the significant differences in the two methods, the effects of microwave oven (MWO) interference are quite different on systems employing these techniques.

This paper describes MWO interference and presents a model which is useful in predicting WLAN reliability. The mechanisms by which the interference disrupts system performance for DSSS and FHSS are described separately. Finally, quantitative results showing packet error rate (PER) under varying levels of interference and packet length are presented and discussed.

Summary

This paper describes the results of an analysis of the effects of varying packet length and interference level on the reliability of WLANs in the presence of microwave oven (MWO) interference. There are four different aspects of this analysis.

Section I deals with modeling interference from microwave ovens. The results of an NTIA report on interference from MWO in the 2.4 GHz ISM band are summarized along with some relevant journal articles. A model of MWO interference presented by Motorola before the IEEE 802.11 WLAN Working Group is discussed. A MWO can be effectively modeled as a swept narrowband jammer with a 50% duty cycle. The resulting interference is synchronized to the 60 Hz AC power line voltage due to the fact that the magnetron power supplies are only half wave rectified.

Section II includes a basic review of the performance of FHSS systems in the presence of narrow band jammers. FHSS systems combat MWO interference by avoiding it. Performance curves are presented which show Packet Error Rate (PER) as a function of both packet length and interference level. Based on the model presented, it is shown that the best line of defense for an FHSS system is a short packet length. This will permit the successful transmission of smaller packets between bursts of interference.

Section III extends this discussion to DSSS systems. DSSS systems have wide occupied bandwidths. This increases the probability that MWO interference will fall "in band". However, the effect of processing gain and the underlying modulation method must be considered. The DBPSK/DQPSK modulation method employed in DSSS radios is considerably more robust than the 2FSK/4FSK method employed by IEEE 802.11 FHSS systems. In addition, the despreading process spreads the bulk jammer power out of band, giving an additional 10 dB improvement in radio performance over non-spread methods. The remaining in-band noise is incoherent white noise. DSSS systems deal with MWO interference by suppressing it, not by avoiding it.

Section IV summarizes the data and provides an interpretation. The results demonstrate that FHSS receivers can transmit short packets (100 - 200 bytes) even in even a very noisy environment. However, when using longer packets (1000 bytes), FHSS systems require a signal strength of 16 to 17 dB above peak interference levels to achieve reliable operation in the presence of MWO interference when operating at 1 Mbps. This effect is even more pronounced when operating at 2 Mbps.

By contrast, packet error rates can be high even for short packets when interference levels exceed signal strength in DSSS systems. Once signal power is roughly equal to jammer power, the DSSS systems can provide reliable operation, regardless of packet length. A DSSS system can reliably receive 1000 byte packets with a signal-to-jammer power ratio of roughly 0 dB, based on the analysis presented. Experience has shown that DSSS systems can operate reliably even in very close proximity to a microwave oven. Analysis such as this provide a good framework for discussion of the MWO interference question, but the most convincing method is a side-by-side test of FHSS and DSSS systems in the presence of an operating microwave oven.

Section I: Model of Microwave Oven Interference

The results of extensive measurements of interference form fourteen different microwave ovens were summarized in a two volume NTIA report [1,2]. The report demonstrates that the interference has roughly a 50% duty cycle with a 16.7 msec period. This is due to the fact that the magnetrons in the ovens are driven by 60 Hz AC power and are active during only half of the sinusoidal line voltage cycle.

Frequency domain measurement of one of the tested MWO is shown in Figure I-1. The measurements were taken using a spectrum analyzer in the "max hold" mode. Peak levels and interference bandwidth vary considerably among ovens from different manufacturers.
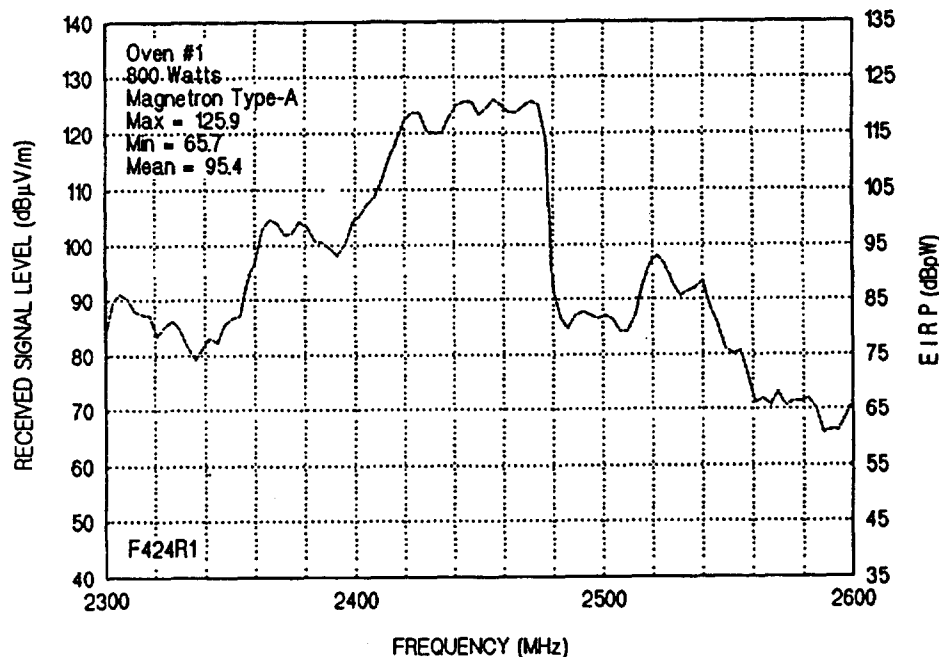
Figure I-1 "Max-Hold" Amplitude vs. Frequency Plot of MWO Interference from NTIA report

The results of the NTIA tests are informative, but the "max hold" frequency domain measurements give an overly pessimistic view of the MWO interference problem. Subsequent measurements [3] using spectrographic techniques show that the instantaneous interference is actually very narrow band. Further, the frequency is swept over a significant portion of the ISM band as the power line voltage across the magnetron varies on each positive half cycle of the 60 Hz sinusoid.

A representation of a spectrographic plot is shown in Figure I-2. Of critical importance are the swept frequency range (f_{swept}) and channel dwell time (t_{dwell}). It has been pointed out that any time an FHSS radio dwells on a channel within the range of swept frequencies for more than 16.7 msec, it will be hit at least twice by interference [4]. As previously mentioned, f_{sweep} varies considerably among ovens from different manufacturers.
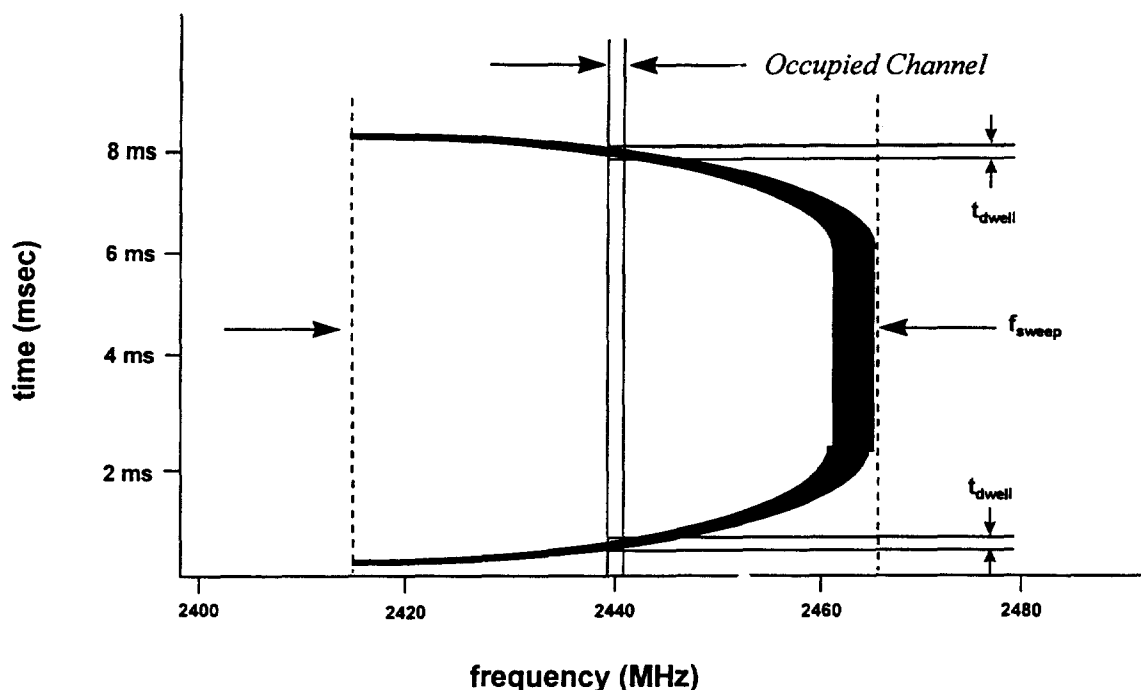
Figure I-2 Spectrographic Plot of Microwave Oven Interfernce

In order to estimate the effects of packet length on system throughput for IEEE802.11 WLAN's, the foregoing characteristics of MWO interference have been incorporated into a simple but useful model [4]. The range and rate of frequency sweep determine channel dwell time, t_{dwell}. Even when operating in the presence of FHSS systems having a relatively narrow occupied bandwidth, t_{dwell} is long enough to ensure that multiple bits will be jammed as the MWO interference sweeps through a given channel. Worst case assumptions would be a swept frequency range of the entire 83 MHz of the 2.4 GHz ISM band over 0.8 msec (10% of the 8 msec "on" time for the magnetron). Assuming a channel width of 1 MHz and 80 separate non-overlapping channels, the number of corrupted bits would be:

$$t_{dwell} \quad = 0.8 \text{ msec} / 80 \text{ channels}$$
$$= 10 \text{ usec}$$

$$\text{\# exposed bits} \quad = 1 \text{ Mbps} * 10 \text{ usec}$$
$$= 10 \text{ bits}$$

Typical channels dwell times are much longer for DSSS systems because the occupied channnle width is significantly larger (20 MHz for DSSS compared to 1 MHz for FHSS). This simple analysis demonstrates that the channel dwell time is sufficient even under worst case conditions to for several bits to be exposed to interference. Typical swept frequency range for domestic microwave ovens is about 50 MHz.
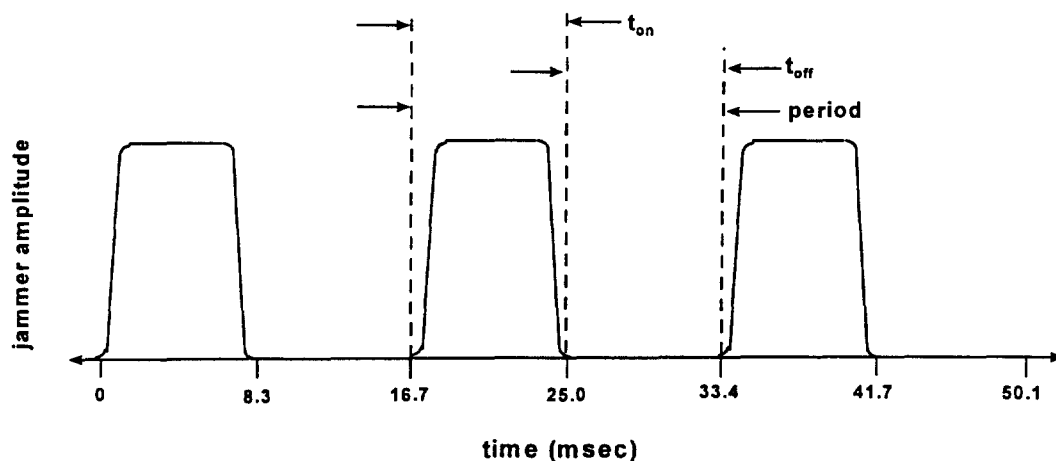
Figure I-3   Microwave Oven Magnetron Duty Cycle

In summary, MWO interference can be characterized as a swept narrowband jammer having a swept frequency range, f_{sweep}, and a channel dwell time, t_{dwell} . The jammer is active over 50% of 60 Hz power line cycle and, therefore, has a period of 16.7 msec. Further, due to the fact that the jammer frequency sweeps on both the *on/off* and *off/on* transients, an individual channel lying within the range of swept frequency will experience two periods of jamming on each cycle of the 60 Hz power line voltage as shown in Figure I-4.
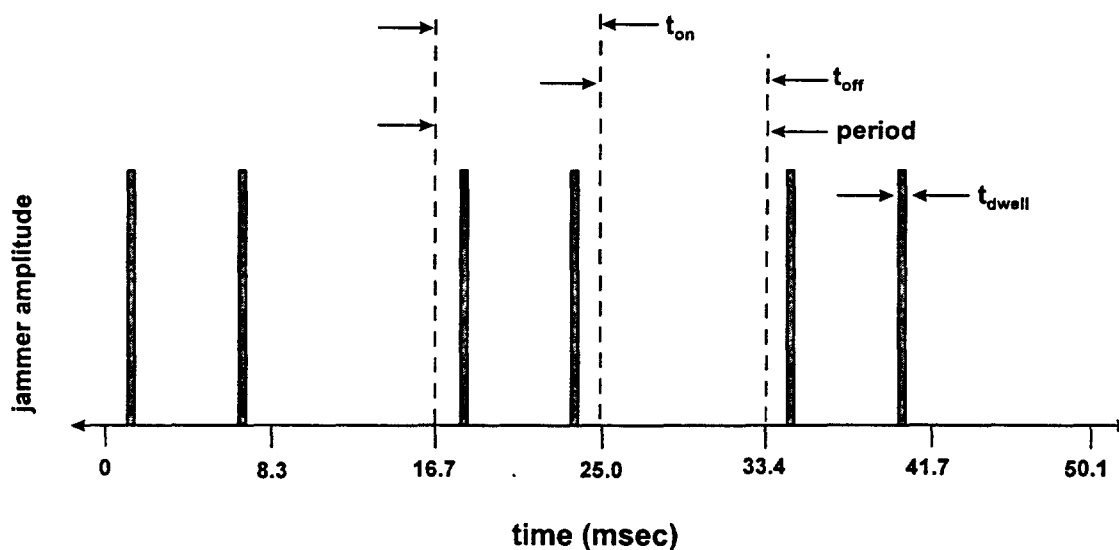
Figure I-4   Microwave Oven Interference in Single FHSS 1 MHz Channel

This model provides a good starting point from which to analyze the effects of MWO interference. In practice, the picture is obscured by the fact that the magnetron initially pulses as the voltage starts to ramp up on the half sine wave. It also pulses as the magnetron shuts down on the falling edge of the power line voltage sine wave. In addition, swept frequency and

radiated emission levels vary as a function of oven load. Nevertheless, this basic model provides a means of analyzing the effects of hop rate and packet length.

Section II: FHSS Systems and Microwave Oven Interference

FHSS systems which operate in accordance with FCC Part 15 rules (15.247) must divide the 83.5 MHz of the ISM band into at least 75 separate channels, with each channel having a maximum width of 1 MHz. The utilization for each channel cannot exceed 400 msec in any 30 second period. Therefore, each channel must get equal utilization when averaged over a 30 second period.

FHSS Modulation Method

IEEE802.11 FHSS systems operate at 2 Mbps using 4-level Frequency Shift Keyed (4FSK) modulation, and 1 Mbps using 2-level FSK (2FSK) modulation. In order to fit 1 or 2 Mbps into a 1 MHz channel, an extremely low modulation index (h) is used. Modulation index is defined as:

$$h = \Delta F / R$$

where h = modulation index
ΔF = frequency deviation between mark and space
R = data rate (bps)

The modulation index is 0.32 for 2FSK and 0.16 for 4FSK. Bit error rates for IEEE802.11 2FSK and 4FSK are shown in Figure II-1. In order to provide 1 and 2 Mbps speed through a 1 MHz occupied bandwidth, extremely narrow frequency deviations were used. The result is a very high signal strength (Eb/No) is required to achieve reliable operation, as measured by Bit Error Rate (BER).
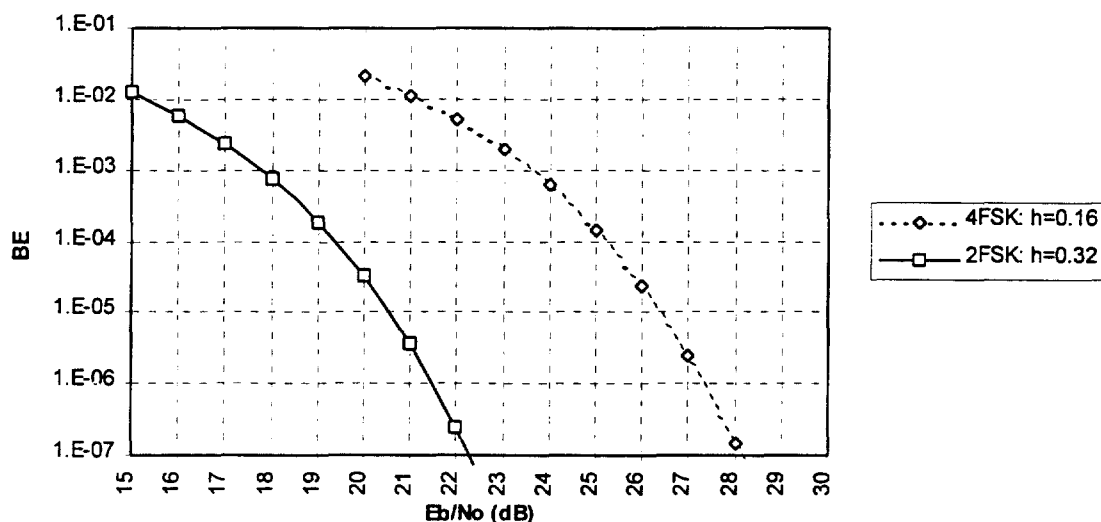
Figure II-1 Bit Error Rate as a Function of Eb/No for 2 and 4 Level FSK

If the bit errors within a packet were uncorrelated random events, extending the results for bit error rate (BER) to packet error rate (PER) would be a straightforward matter. However, it has now been shown that the interference from microwave ovens is not purely random in nature. In addition, the systems under consideration are decidedly slow hoppers. Therefore all bits within a packet are transmitted on the same frequency. Bit errors within a packet are therefore not uncorrelated events.

In order to perform an analysis of throughput, some assumptions about swept frequency range and sweep rate must be made. Data gathered from lab tests at Harris Semiconductor, as well as published test data [1,2] indicate that the range of swept frequency for domestically produced microwave ovens is about 50 MHz. A sweep rate of 0.8 msec for the on/off and off/on transients is also assumed. This is consistent with the model described above [4], as well as published spectrographic data [3].

For the purpose of this analysis, it is assumed that the MWO interference can be treated as white noise within the relatively narrow occupied channel (1 MHz) of an FHSS radio. Magnetrons are inherently narrowband devices due to the geometry of the tuned cavities. However, under loading the resonant bandwidth, or Q, expands significantly and has an instantaneous bandwidth on the order of 500 kHz. In addition, the MWO interference is swept during off/on and on/off transients (described in Section I) and the exact instantaneous location within the occupied channel is purely random. The low modulation indicies for 2FSK and 4FSK, 0.32 and 0.16, result in extremely high symbol cross-correlation coefficients (ρ), 0.85 and 0.95 respectively. For noncoherent receivers, the symbol cross-correlation is computed by:

$$\rho = \frac{\sin\pi h}{\pi h}$$

where p = sysmbol cross correlation coefficient
        h = modulation index

High symbol cross correlation will cause any in-band interference to have approximately the same effect on both the mark and space decision variables, regardless of its precise location within the occupied channel.

It is further assumed that a single bit error will cause the CRC to indicate a bad packet, resulting in a packet error. Based on the assumption that a single bit error results in a packet error, the effects of the scrambler can be neglected. The only means of avoiding packet errors is to avoid periods of interference, or to overcome it with sufficient signal strength.

MWO Interaction with FHSS Signals: Analysis by Conditional Probabilities

PER can be estimated by the use of conditional probabilities. As shown in Figure II-2, the occupied channel of a FHSS radio will fall into one of three regions relative to the MWO interference. If the occupied channel falls outside the range of swept frequency (f$_{sweep}$), no interference will occur (Condition A). If the occupied channel falls within the range of swept frequency, the receiver will either experience intermittent periods of interference during magnetron transients (Condition B), or prolonged periods of interference (Condition C). For Conditions B and C, the probability of successful transmission is a function of packet length [4]. This model is described briefly below and in greater detail in the Appendix.
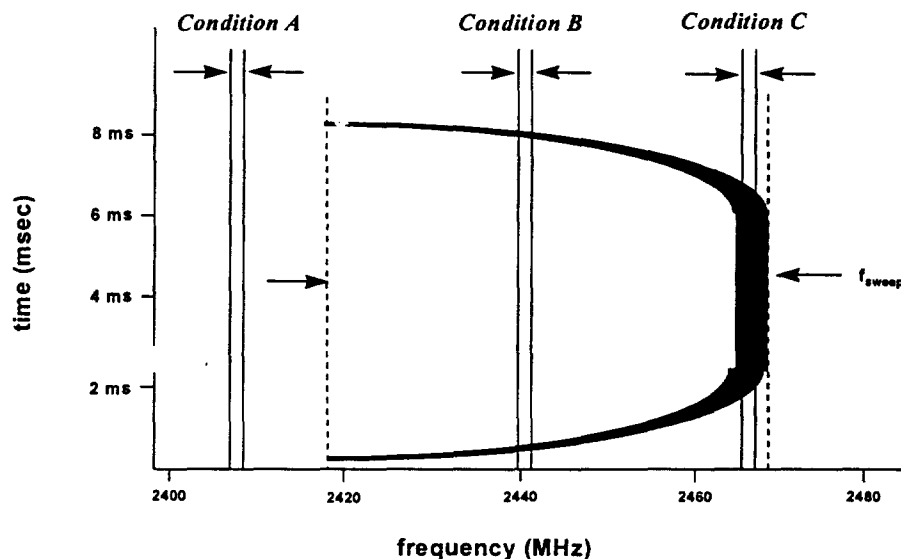

Figure II-2 Possible Conditions for Occupied Channel in Presence of MWO Interference

There are three possible conditions for the occupied channel in the presence of MWO interference:

Condition A: Occupied Channel lies outside the range of swept frequency. In this case, data transmission is assumed to be error free.

Condition B: Occupied Channel lies within the range of swept frequency, but is jammed only during on/off and off/on transients of the magnetron.

Condition C: Occupied Channel lies within the range of swept frequency, and the occupied channel lies on same frequency as magnetron steady state operation.

These conditions are exhaustive and mutually exclusive. Therefore:

$$P_A + P_B + P_C = 1$$

Condition A

In this situation, the FHSS channel lies outside the range of occupied frequency. The likelihood of this condition (P_A) is:

$$P_A = (83.5 \text{ MHz} - f_{sweep}) / 83.5 \text{ MHz}$$

For this condition, data transmission is assumed to be error free. The implication is that there is some minimum level of system reliability, regardless of the level of interference.

Condition B

For Condition B, the occupied channel lies within the range of swept frequency, but experiences only brief periods of interference during off/on and on/off transients of the magnetron. It is further assumed that the interference from the magnetron is <1 MHz once it reaches a steady state condition. The probability of Condition ? (P_B) is therefore:

$$P_B = (f_{sweep} - 1 \text{ MHz}) / 83.5 \text{ MHz}$$

A time domain representation of microwave interference for Condition B is shown in Figure II-3. From this figure, it becomes apparent that packet length is the dominant factor which determines PER under this condition. Packets longer than 9.2 msec have no chance of avoiding interference.
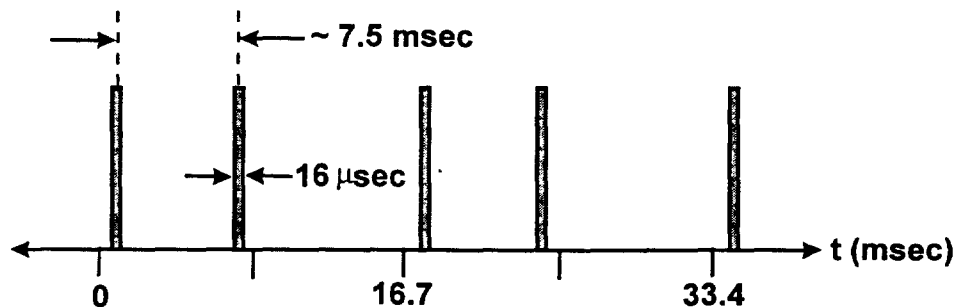

Figure II-3 Time Domain Representation of MWO Interference for Condition B

Condition C

In this case, the occupied channel for the radio coincides with the steady state operating frequency of the MWO magnetron. This is the worst case condition, due to the relatively large

duty cycle of interference in this channel, as shown in Figure II-4. Fortunately, the severity of this condition is mitigated by the relatively low probability of its occurrence. The MWO is modeled as a narrowband jammer once it reaches steady state after the off/on transient. It has a bandwidth < 1 MHz, and therefore can only jam a single channel. The probability of Condition C (P_C) is:
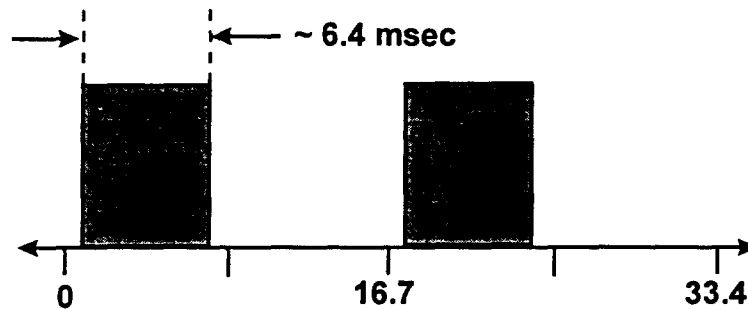
$$P_C = 1 \text{ MHz} / 83.5 \text{ MHz}$$

Figure II-4 Time Domain Representation of MWO Interference for Condition C

FHSS Receiver Sensitivity

Inclusion of the effect of receiver sensitivity requires an additional conditioned probability. The model must include an estimate of the number of bits (n) exposed to interference (but not necessarily erroneous) when transmitted during burst of jammer energy. PER For Condition B is then estimated as follows:

$$PER_B = P_B * P_{MWOB} * [1 - (1 - P_e)^n]$$

where:

PER_B = Packet Error Rate given Condition B
P_B = Probability of Condition B
P_{MWOB} = Probability of encountering MWO interference given Condition B
P_e = Probability of bit error
n = estimate of number of corrupted bits

Conditions A, B, and C are mutually exclusive and exhaustive. Total PER is therefore the sum of the PER under each of the three conditions (PER under Condition A is assumed to be zero). For a more detailed description method employed to include receiver sensitivity, see the Appendix. PER has been computed as a function of relative jammer power (Eb/Jo) for several values of packet length at 1 Mbps and 2 Mbps, as shown in Figures II-5 and II-6 respectively.
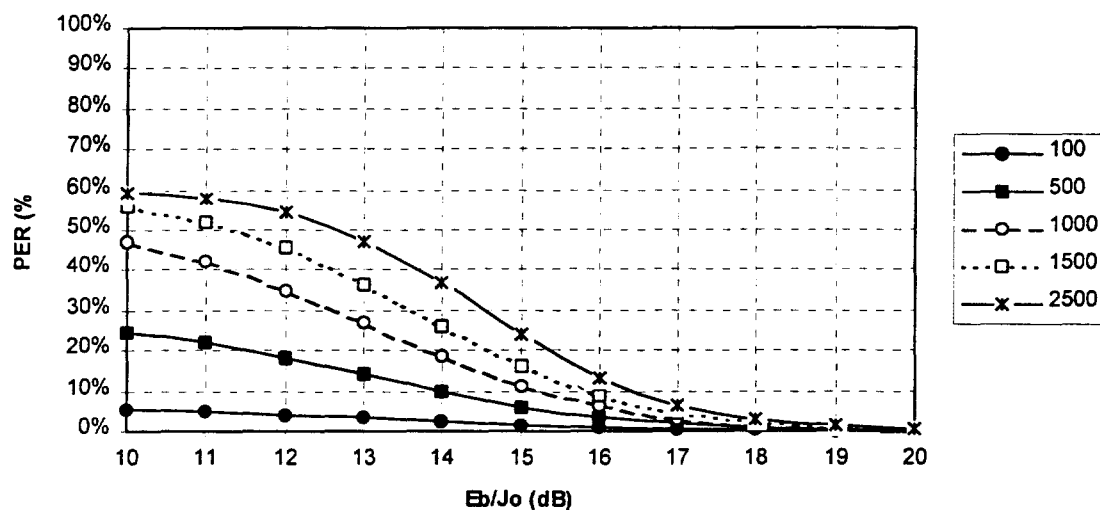
Figure II-5 FHSS PER as a Function of Packet Length (bytes) and Relative Jammer Power @ 1 Mbps
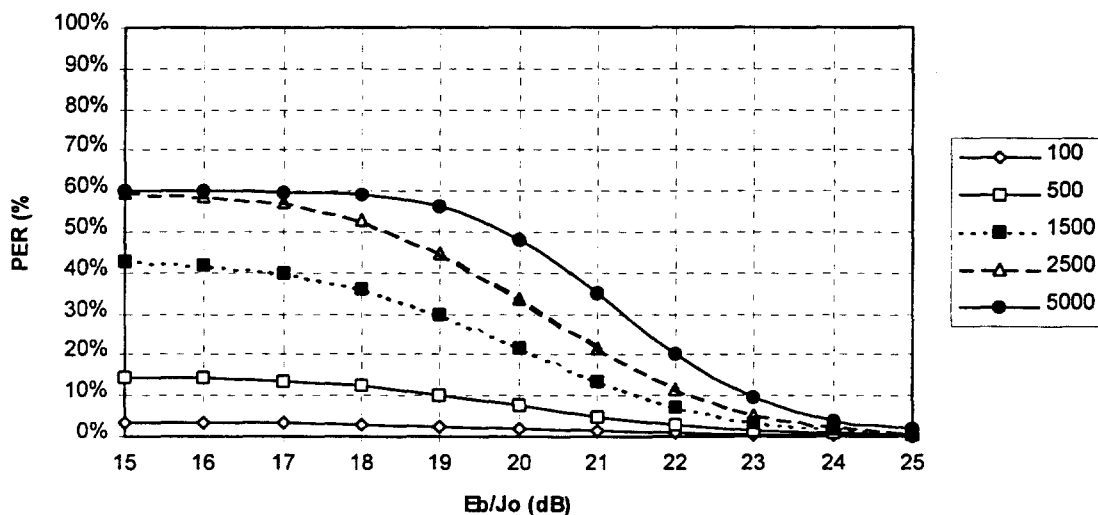

Figure II-6 FHSS PER as a Function of Packet Length (bytes) and Relative Jammer Power @ 2 Mbps

These results demonstrate that the signal strength for an FHSS radio must exceed the interference from a MWO by about 16 dB when operating in the 1 Mbps mode before reliable packet reception (PER < 10%) is possible for longer packets. However, shorter packets (100 to 200 bytes) can be received reliably even in a high interference environment because of their ability to avoid bursts of jammer energy. The difference between error rates for long and short packets is even more pronounced at 2 Mbps. Short packets are still able to avoid MWO jammer bursts, however longer packets require as much as 22 dB Eb/Jo for reliable transmission.

Section III: DSSS Systems and Microwave Oven Interference

Operating rules for DSSS systems in the ISM band are covered under the same section of the FCC regulations as the FHSS systems (15.247). By these regulations, DSSS systems do not have an occupied bandwidth restriction but must have a minimum of 10 dB processing gain. IEEE 802.11 DSSS systems have an occupied bandwidth of roughly 20 MHz. Processing gain is realized by modulating each data bit with an 11 bit Barker code (pseudo random sequence). Processing gain is therefore 11:1, or 10.4 dB.

DSSS Modulation Method

IEEE802.11 DSSS systems employ Differential Binary Phase Shift Keying (DBPSK) and Differential Quadrature Phase Shift Keying (DQPSK) for 1 Mbps and 2 Mbps modulation, repectively. BER curves for these modulation methods are shown in Figure III-1. Note that the required Eb/No for a BER of 10^{-5} is 10 dB for DBPSK and 12 dB for DQPSK.
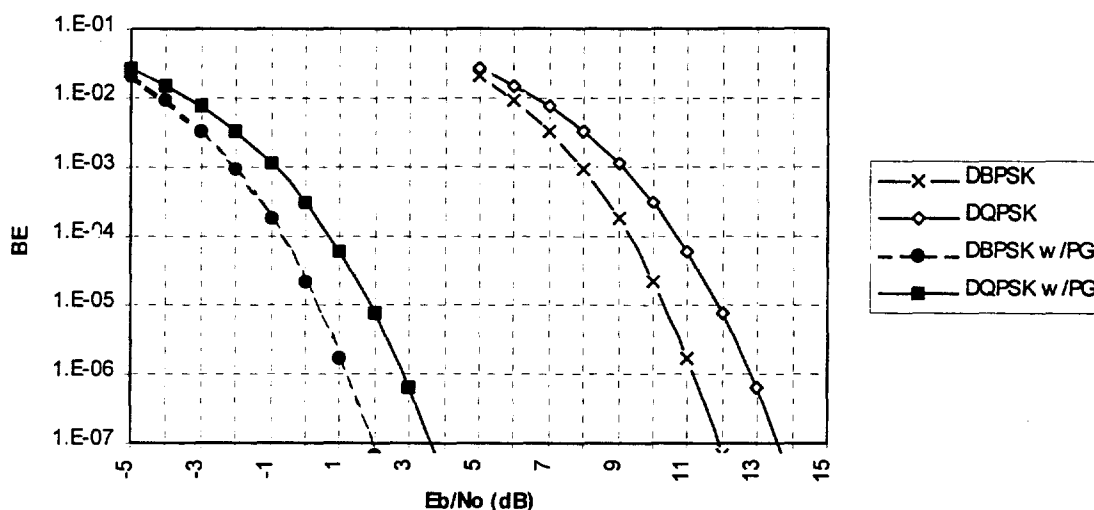

Figure III-1 Bit Error Rate as a Function of Eb/No for DBPSK/DQPSK and DBPSK/DQPSK with Processing Gain

Aside from a more power efficient modulation method, DSSS systems also provide processing gain against narrow band jammers, including microwave ovens. As described above, the level of processing gain is 10 dB. There are two main effects of the "despreading process":

    a. Narrowband interference is reduced by a factor of 10 dB

    b. Remaining interference is converted to wideband white noise

The first effect, reduction of interference power, is depicted in Figure III-2 by the curves at the extreme left of the plot. These are simply the BER curves for DBPSK abd DQPSK shifted to the left by 10 dB to indicate the performance improvement in the presence of a narrow band jammer. The second effect, conversion of narrowband interference into white noise, is significant because

it facilitates analysis of system performance. A discussion of the mechanics of DSSS processing gain is presented by Dixon [6].

Microwave Oven Interference Effects on DSSS Signals

The interaction of MWO interference with DSSS signals is quite different than with FHSS signals. Unlike FHSS radios, DSSS radios are not frequency agile. They also have a much greater occupied bandwidth (20 MHz as compared to only 1 MHz for the FHSS radios). While a DSSS radio might be tuned to avoid all or most of the interference in a given scenario, it is equally likely that it could be tuned so that most of the interference falls in-band.

The latter situation is the "worst case" and is the subject of this analysis. It is assumed that the stable operating frequency of the MWO is in the high end of the occupied channel for the radio as shown in Figure III-2. Under this condition, all of the energy for emitted from the MWO once the magnetron frequency stabilizes and most of the emission during the transient condition will fall in band. This is a "worst case" condition for the DS system.
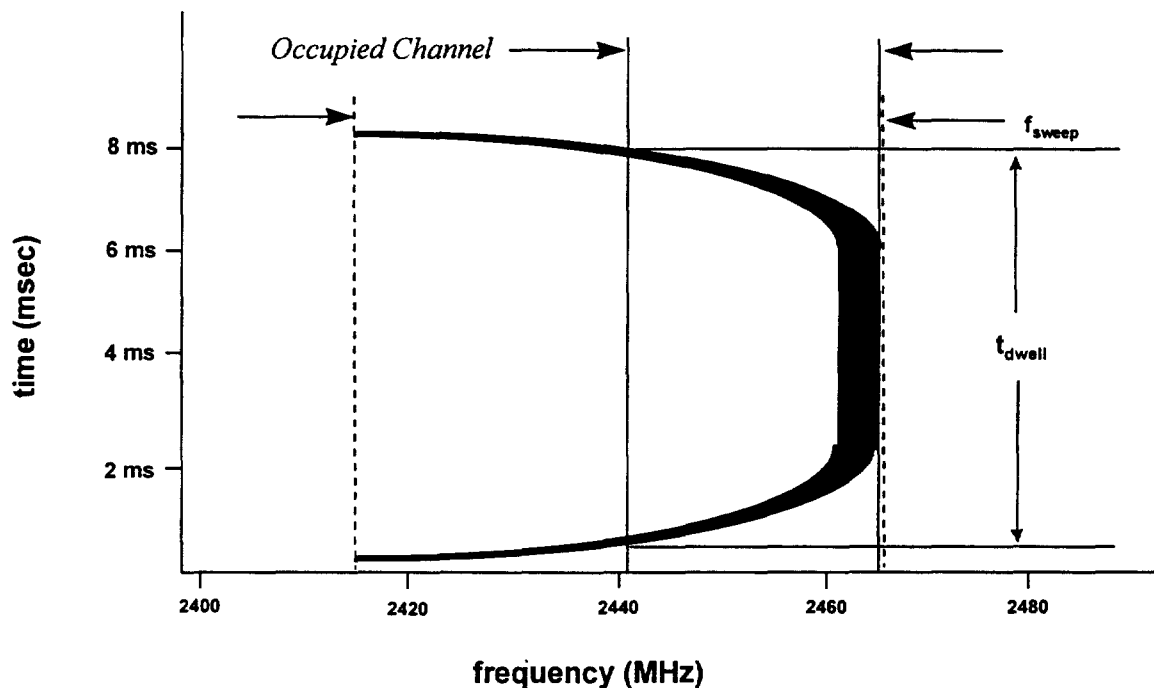

Figure III-2 DSSS Occupied Channel in Presence of MWO Interference

The result of a scenario such as this is that the MWO interference is present in the occupied channel for a period of time which roughly coincides with the magnetron duty cycle. This is analogous to Condition C for the FHSS system described in Section II above, with the exception that the probability of its occurrence is 100% under the stated conditions.
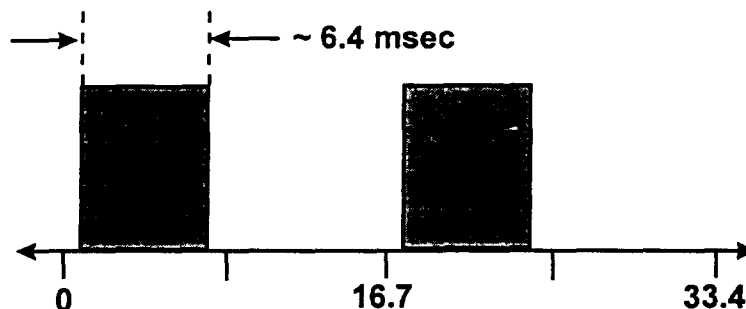
**Figure III-3   Time Domain Representation of "Worst Case"
MWO Interference in a DSSS System**

DSSS Receiver Sensitivity

The DSSS case is a bit more straight forward than the FHSS case, because there are no conditioned probabilities. If the DSSS receiver is tuned as shown in Figure III-2, the effect of MWO interference is computed in exactly that same manner ืs Condition C for the FHSS case, with the exception that the BER curves shown in Figure III-1 are used, and the probability of the occurrence of this condition is 100%. Again, the model must include an estimate of the number of bits (n) exposed to interference (but not necessarily erroneous) when transmitted during burst of jammer energy. PER is then estimated as follows:

$$PER = P_{MWO} * [1 - (1 - P_e)^n]$$

where:

PER   = Packet Error Rate
P_{MWO} = Probability of encountering MWO
P_e = Probability ืf bit error (assuming 10 dB Processing Gain)
n   = estimate of number of corrupted bits

PER has been computed as a function of relative jammer power (Eb/Jo) for several values of packet length at 1 Mbps and 2 Mbps, as shown in Figures III-4 and III-5 respectively.
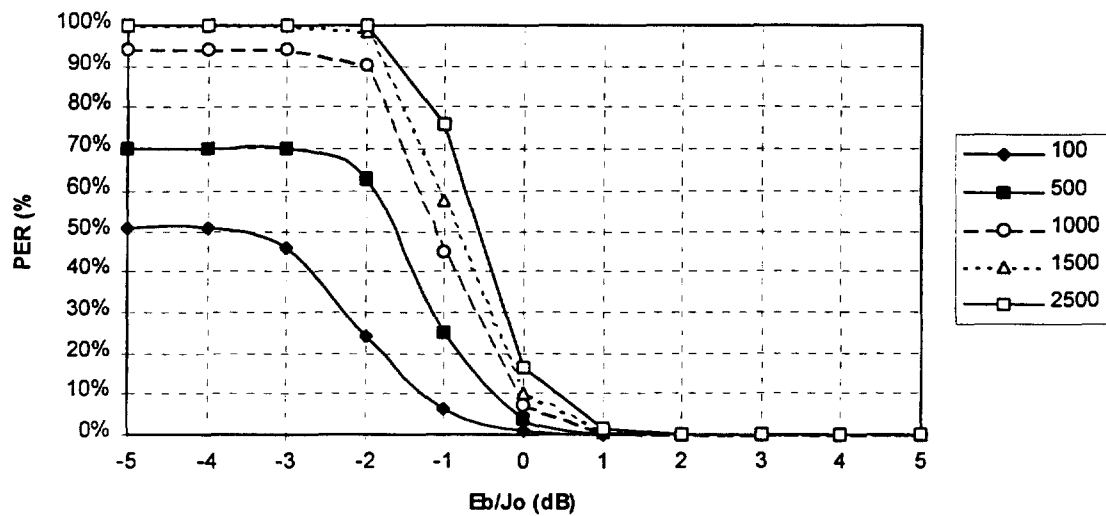
Figure III-4 DSSS PER as a Function of Packet Length (bytes) and Relative Jammer Power @ 1 Mbps
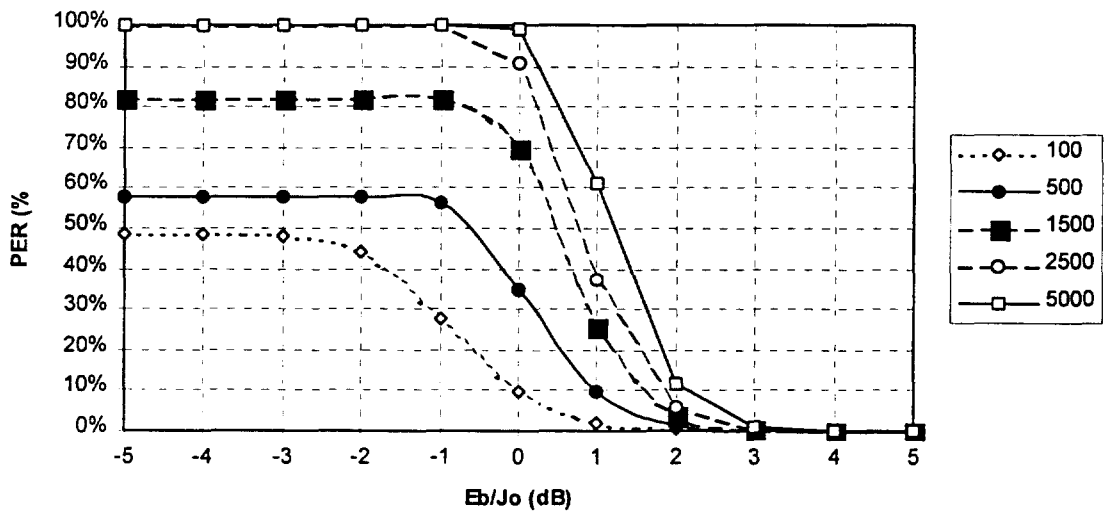
Figure III-5 DSSS PER as a Function of Packet Length (bytes) and Relative Jammer Power @ 2 Mbps

Reliability of the DSSS system is far less dependent on packet length. For extremely high levels of interference, even short packets have a high error rate (50%). However, PER for 100 byte packets drops below 10% with Eb/Jo at about -1dB. For longer packets (2500 bytes), PER drops below 10% with Eb/Jo at 0.5 dB. The reason behind this effect is the DS system does not *avoid* the jammer, it *suppresses* it. Experience has shown that DSSS receivers can operate in very close proximity to microwave ovens and still maintain reasonable throughput.

Section IV: Comparison of Results

The results for both the DSSS and FHSS systems in the presence of MWO interference is summarized in Table IV-1.

Packet Length (bytes)	1 Mbps (Eb/Jo @10% PER)			2 Mbps (Eb/Jo @10% PER)	
	DSSS	**FHSS**		**DSSS**	**FHSS**
100	-1.0	*<10% PER*		0	*<10% PER*
500	-0.5	14		1	19
1000	0.0	15		1.25	21
1500	0.0	16		1.5	21.5
2500	0.5	16.5		2	22
5000	0.75	17		2	23

Table IV - 1   Required Eb/Jo to Achieve 10% Packet Error Rate

By virtue of the narrow occupied bandwidth, FHSS systems are able to avoid interference with short packet lengths regardless of the interference level. Note that the PER remains below 10% for all levels of interference power with short packets (100 bytes) for both the 1 Mbps and 2 Mbps FHSS cases. However, in order to achieve reliable operation with longer packets, a lot of signal energy is required at the receiver.

As packet length increases, the FHSS system can no longer avoid interference. Instead, it must now overpower it. The low modulation indices for both 2FSK at 1 Mbps and, in particular, 4FSK at 2 Mbps drive the signal strength requirement in this situation. For a packet length of 1000 bytes, the FHSS system requires 15 dB Eb/Jo to achieve a 10% PER at 1 Mpbs, and 21 dB Eb/Jo to reach 10% PER at 2 Mbps.

The DSSS system has a much higher occupied bandwidth and is not frequency agile. It can therefore be tuned to a frequency where nearly all of the MWO interference falls within the occupied channel. Interference avoidance is not possible for DSSS systems in such a situation. This is offset by two features of IEEE802.11 systems:

   a. The DBPSK/DQPSK modulation method is more power efficient than the 2FSK/4FSK modulation employed by FHSS systems

   b. IEEE802.11 DSSS systems reject about 90% of the energy of a narrow band jammer such as a microwave oven

Table IV-1 shows that PER for DSSS systems can be very high even for short packets when jammer power exceeds signal strength. However, once signal power is at or above jammer power, the DSSS system provides reliable operation regardless of packet length. In terms of the real world environment, experience has shown the DSSS systems can operate reliably in very close proximity of a microwave oven.

This analysis studies the effects of MWO interference in isolation. There are other effects such as signal attenuation and multipath that are of at least equal importance in terms of determining overall WLAN reliability. This paper represents an attempt to provide a framework for discussing the MWO interference issue in a quantitative manner. As always, the best means determining which system is better in a given application is via side-by-side system testing.

References

1. P.E. Gawthrop, F.H. Sanders, J.J. Sell, "Radio Spectrum Measurements of Individual Microwave Ovens", NTIA Report 94-303-1.

2. P.E. Gawthrop, F.H. Sanders, J.J. Sell, "Radio Spectrum Measurements of Individual Microwave Ovens", NTIA Report 94-303-2.

3. J. Horne, S. Vasudevan, "Modeling and Mitigation of Interference in the 2.4 GHz ISM Band", Applied Microwaves & Wireless, March/April 1997, pp. 59-71.

4. Jim McDonald, Motorola Inc., "Recommendations for 2.4 GHz Frequency Hop Packet or Fragment Length", IEEE Document P802.11-94/109, May 1994.

5. A. Kamerman, N. Erkocevic, "Microwave Oven Interference on Wireless LANs Operating in the 2.4 GHz ISM Band", The 8th International Symposium on Personal Indoor and Mobile Radio Communications, Helsinki, Finland, September 1997.

6. Robert C. Dixon, "Spread Spectrum Systems, 3rd Edition", John Wiley & Sons, 1994, pp. 36-44.

7. John G. Proakis, "Digital Communications, 2nd Edition", McGraw-Hill, 1989, pp. 851-859.

Appendix A: Model of MWO Interference on FHSS Radios

This analysis is based on a few simple conditional probabilities. It is assumed that data transmission is error free in the absence of MWO interference. It further assumes that one bit error will cause a packet error. In that case, the CRC check will fail and the packet is invalidated. Given the assumption that one bit error will cause a packet error, the effects of scrambling can be neglected. The occurrence of multiple errors at the output of the data descrambler (one error for each term in the polynomial) in the event of one bit error at the input does not change the probability of a packet error.
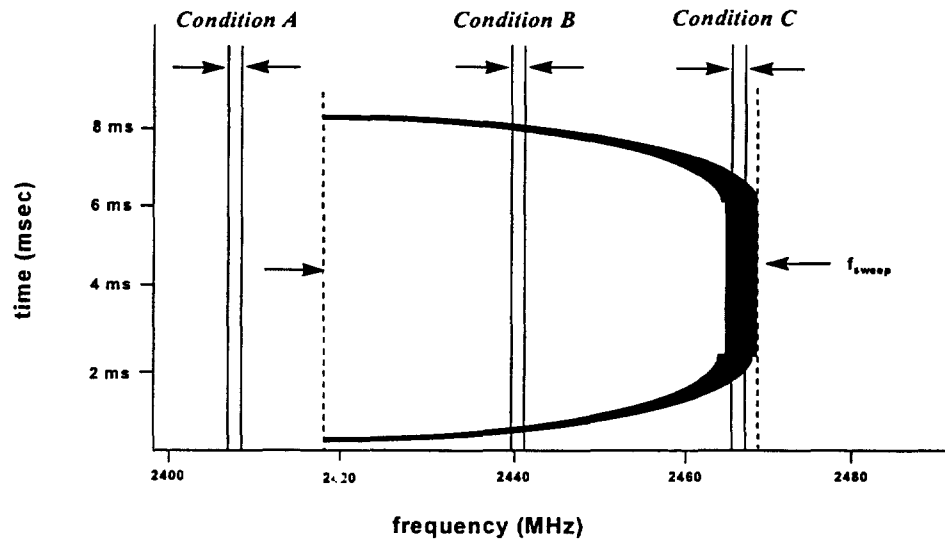

Figure A-1 Possible Conditions for Occupied Channel in Presence of MWO Interference

Condition A: Occupied Channel is Outside Range of Swept Frequency

FCC regulations (15.247) require that all frequencies in the 2.4 GHz be utilized equally. Therefore, the occupied frequency is a uniform random variable in the range of 2.4000 - 2.4835 GHz. Referring to Figure A-1, the probability of occurrence for Condition A (P_A) is given by:

$$P_A = (83.5 \text{ MHz} - f_{sweep}) / 83.5 \text{ MHz} \qquad (A.1)$$

It is assumed that transmission is error free in the absence of MWO interference. Therefore, if the occupied channel is outside the range of swept frequency (f_{sweep}) no dropped packets will occur. The packet error rate for Condition A (PER_A) is:

$$PER_A = 0 \qquad (A.2)$$

For $f_{sweep} = 50$ MHz:

$$P_A = (83.5 \text{ MHz} - 50 \text{ MHz}) / 83.5 \text{ MHz} = 40.1\%$$

This value establishes an absolute minimum level of system reliability. Regardless of packet length, packets transmitted on channels outside the range of swept frequency will be successfully received.

Condition B: ***Occupied Channel is Within Range of Swept Frequency and Experiences Interference on Magnetron Transients***

In this case, successful transmission relies on the ability to transmit packets between bursts of MWO interference. If the packet is longer than the time gap between bursts of interference, successful transmission is not possible. If the packet is shorter than the gap duration as shown in Figure A-2, the start of transmission (t_{start}) must be such that the packet can be completely sent before the next burst.
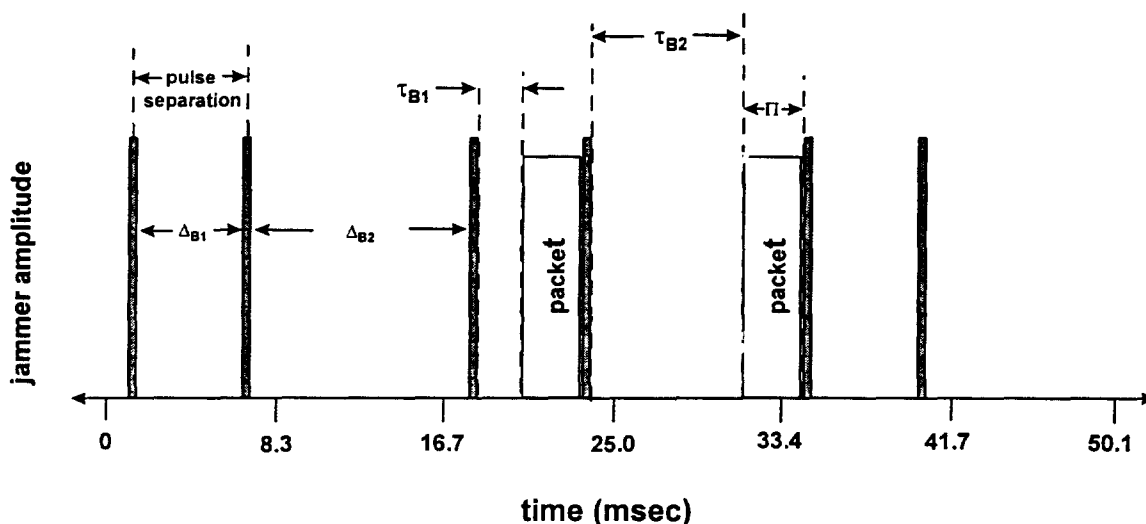

Figure A-2   Time Gaps between MWO Interference Pulses (Condition B)

It is assumed that the bandwidth of emissions from the MWO is about 1 MHz once it reaches steady state operation. The probability of occurrence for Condition B (P_B) is:

$$P_B \quad = (f_{sweep} - 1 \text{ MHz}) / \ 83.5 \text{ MHz} \qquad (A.2)$$

As shown in Figure A-2, there are two distinct gaps, Δ_{B1} and Δ_{B2}, to consider. The window of starting time for successful transmission for Gap B1 (τ_{B1}) is:

$$\tau_{B1} \quad = \Delta_{B1} - \Pi \qquad (A.3)$$

where:

$$\begin{aligned}
\tau_{B1} \quad &= \text{window of start of transmission in Gap B1} \\
\Delta_{B1} \quad &= \text{Gap B1 duration} \\
\Pi \quad &= \text{packet length (time)}
\end{aligned}$$

The computation for τ_{B2} is identical. The probability of packer error given that Condition B holds (PER$_B$), is:

$$PER_B = 1 - [(\tau_{B1} + \tau_{B2}) / 16.7 \text{ msec}] \qquad (A.4)$$

The time gaps vary slightly over the range of swept frequency. However, for the purposes of this model, this effect is neglected. The time gaps, Δ_{B1} and Δ_{B2}, are treated as constants.

Condition C: *Occupied Channel Frequency is same as Magnetron Steady State Operating Frequency*

The frequency sweeps induced by the off/on and on/off transients of the MWO magnetron are of relatively short duration. After the initial off/on transient, the magnetron frequency achieves steady state and dwells on a particular frequency for about 80% of its duty cycle, or about 6.4 msec, as shown in Figure A-3. For this period, the MWO looks like a relatively stable narrow band jammer. It is assumed that the MWO jams only a single channel during this time. The probability for Condition C (P$_C$) is:

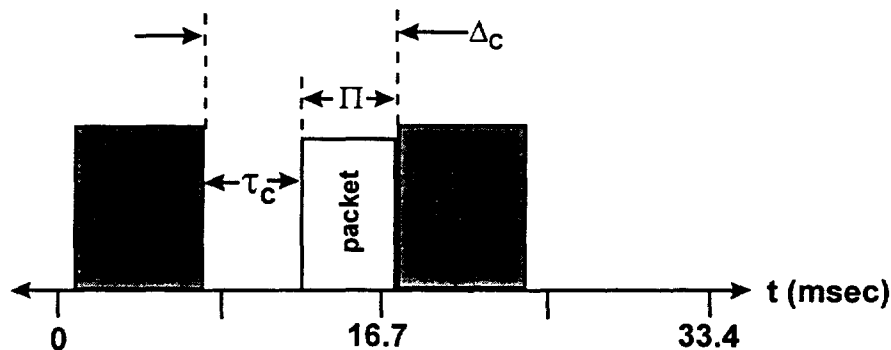$$P_C = 1 \text{ MHz} / 83.5 \text{ MHz} = 0.012 \qquad (A.5)$$

Figure A-3   MWO Interference Pulses (Condition C)

As shown in Figure A-3, there is only a single time gap (Δ_C) to consider. The window of starting time for successful transmission for Gap C (τ_C) is:

$$\tau_C = \Delta_C - \Pi \qquad (A.5)$$

and the and the probability of packet error for Condition C (PER$_C$) is:

$$PER_c = 1 - [(\tau_C) / 16.7 \text{ msec}] \qquad (A.6)$$

Receiver Sensitivity

In order to include the effects of receiver sensitivity, some assumptions about modulation must be made. As described in the main text, 2FSK (h=0.32) and 4FSK (h=0.16) signaling is used. The probability of bit error (P_e) for noncoherent FSK receivers is described by Proakis [7].

In the event that a packet encounters a burst of interference, some number of bits (n) will be corrupted. In this sense, a corrupted bit is one which is transmitted during a burst of interference. It may or may not be received in error. The exact number of corrupted bits is dependent on the packet length (Π), the duration of the interference burst (Ω), and the start-of-transmission time (t) as shown in Figure A-4.
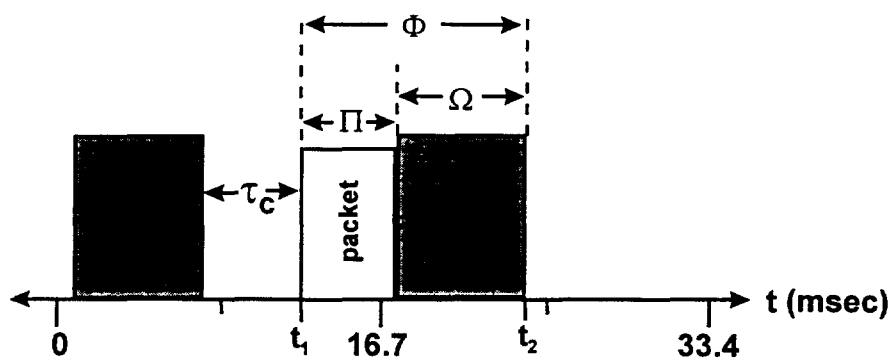

Figure A-4   Packet in Presence of MWO Burst

The number of corrupted bits as a function of start-of-transmission time (t) is shown in Figure A-5. This is actually a correlation of the packet and MWO burst. Given that interference occurs, the expected number of corrupted bits (n) is the average value of the correlation function over the interval for which it is non-zero (t_1 to t_2), as in Figure A-6.
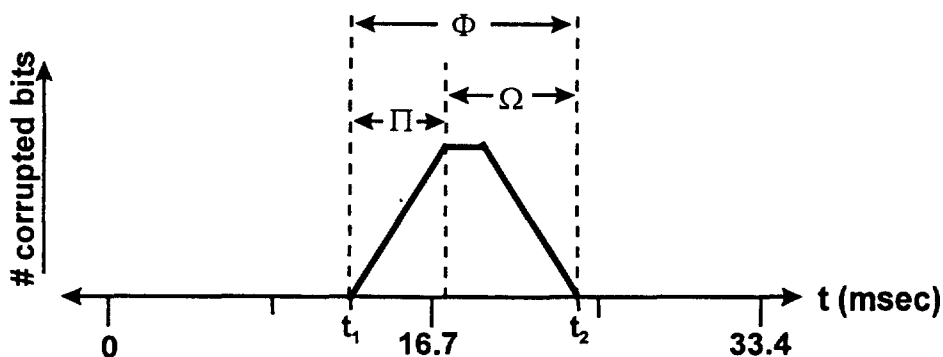

Figure A-5   #Corrupted Bits as Function of Start Time (t)
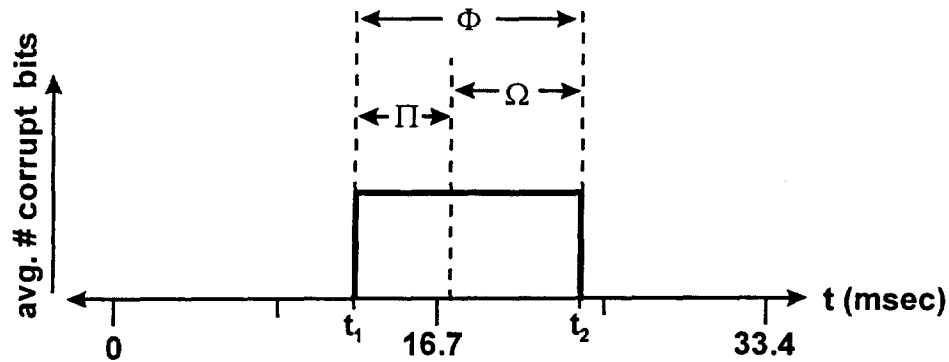
Figure A-6   Average #Corrupted Bits as Function of Start Time (t)

The computation for packer error rate given Condition C (PER_C) is:

$$PER_C = P_C * P_{MWOC} * [\,1 - (\,1 - P_e)^n\,] \qquad (A.7)$$

where:

PER_C = Packet Error Rate given Condition C
P_C = Probability of Condition C
P_{MWOC} = Probability of encountering MWO interference given Condition C
P_e = Probability of bit error
n = estimate of number of corrupted bits

The computation for PER_B is identical to the method shown in (A.7).

Overall Probability of Successful Packet Transmission

Conditions A, B and C are mutually exclusive events. The overall packet error rate is:

$$PER = \{P_A * PER_A\} + \{P_B * PER_B\} + \{P_C * PER_C\} \qquad (A.8)$$